DESY 11-128

Light NMSSM Higgs bosons in SUSY cascade decays at the LHC

Oscar Stål and Georg Weiglein

Deutsches Elektronen-Synchrotron DESY
Notkestraße 85, D–22607 Hamburg, Germany

E-mail: oscar.stal@desy.de, georg.weiglein@desy.de

Abstract: An interesting feature of the next-to-minimal supersymmetric standard model (NMSSM) is that one or more Higgs bosons may be comparably light ($M_{H_i} < M_Z$) without being in conflict with current experimental bounds. Due to a large singlet component, their direct production in standard channels at the Large Hadron Collider (LHC) is suppressed. We demonstrate that there are good prospects for observing such a light Higgs boson in decays of heavy neutralinos and charginos. We consider an example scenario with 20 GeV $< M_{H_1} < M_Z$ and show that a large fraction of the cascade decays of gluinos and squarks involves the production of at least one Higgs boson. Performing a Monte Carlo analysis at the level of fast detector simulation, it is demonstrated how the Higgs signal can be separated from the main backgrounds, giving access to the Yukawa coupling of the Higgs to bottom quarks. Analyzing the resulting $b\bar{b}$ mass spectrum could provide an opportunity for light Higgs boson discovery already with 5 fb^{-1} of LHC data at 7 TeV.

Keywords: Supersymmetry, Higgs bosons, NMSSM, LHC

Contents

1 Introduction

The precise nature of the Higgs mechanism thought to be responsible for electroweak symmetry breaking remains unknown. To discover and study the properties of one or more Higgs bosons is therefore a challenge — and one of the major objectives — for the experiments at the running Large Hadron Collider (LHC). Most of the Higgs boson search strategies to date are designed to probe the Higgs sector of the Standard Model (SM), or its minimal supersymmetric extension (MSSM) [1, 2].

There are several theoretically appealing arguments for weak-scale supersymmetry to be realized in nature: it solves the hierarchy problem of the SM Higgs mass, it enables gauge coupling unification, and with R-parity conservation it also provides a natural dark matter candidate. On the other hand, the realization of weak-scale supersymmetry in terms of the MSSM is not free of theoretical problems, such as the scale for the bilinear μ-parameter entering the MSSM superpotential with positive mass dimension. This parameter has no natural values besides $M_{\rm GUT}$ or zero, while at the same time it must be close to the electroweak scale for a phenomenologically acceptable theory. To solve this problem in an elegant way the MSSM can be extended by a complex scalar singlet, giving the so-called next-to-minimal supersymmetric model (NMSSM). In this model an effective μ-term of

the right size can be generated dynamically from supersymmetry-breaking operators. For a general introduction to the NMSSM we refer to the recent reviews [3, 4].

The NMSSM is characterized by an enlarged Higgs and neutralino sector as compared to the MSSM, giving rise in particular to a richer Higgs phenomenology. While it is well known that in certain scenarios of the MSSM with complex parameters a light Higgs, with mass much below that of the Z boson, is unexcluded by the searches at LEP [5] and the Tevatron [6] (see [7, 8] for recent reevaluations with improved theoretical predictions), such a scenario can occur even more generically in the NMSSM. In order to be compatible with the limits from the LEP Higgs searches, in particular the couplings of such a light Higgs state to gauge bosons must be heavily suppressed. As a consequence of the presence of a Higgs singlet, in the NMSSM such a situation happens whenever a light Higgs state has a sufficiently large singlet component.

The search for a heavier Higgs state with SM-like (or only moderately suppressed) couplings to gauge bosons is complicated in such a scenario by the fact that often the decay of this heavier Higgs state into a pair of lighter Higgses is kinematically open, giving rise to unusual decay signatures and to a large suppression of the standard search channels for a SM-like Higgs. It should be noted in this context that the observation of a decay of a heavier Higgs into a pair of lighter Higgses would provide an opportunity for gaining experimental access to triple-Higgs couplings, which are a crucial ingredient of electroweak symmetry breaking via the Higgs mechanism.

While in the NMSSM the case of a very light pseudo-scalar, $M_{A_1} < 2m_b$, has found considerable attention in the literature, in particular in the context of "ideal" Higgs scenarios [9–14], we will focus in the following on scenarios with a light CP-even boson with 20 GeV $< M_{H_1} < M_Z$. Within the MSSM the best known example of a light Higgs that is unexcluded by the present search limits is the "hole" in the coverage of the CPX benchmark scenario [15] for $M_{H_1} \approx 45$ GeV and moderate values of $\tan\beta$ [5], see [8] for a detailed discussion of the dependence of the unexcluded parameter region on the choice of the various MSSM parameters. It will be difficult to cover this parameter region with the standard search channels at the LHC [16–18]. Various other (non-standard) search channels have been proposed which may provide additional sensitivity in the quest to close this "CPX hole" [16, 19–26].

In our analysis within the NMSSM we will investigate the prospects for the production of light Higgs bosons in cascade decays of heavy SUSY particles at the LHC. Such an analysis, where Higgs bosons are produced in association with — or in decays of — other states of new physics, is necessarily more model-dependent than the Higgs search in SM-like channels. On the other hand, investigating Higgs physics in conjunction with the production of other states of new physics offers additional experimental opportunities and may also be more realistic, in the sense that in order to extract a Higgs signal backgrounds both from SM-type and new physics processes have to be considered. In the case of the MSSM with real parameters, for a Higgs with a mass above the LEP limit for a SM Higgs of 114.4 GeV [27], a detailed experimental study for Higgs boson production in a SUSY cascade has been carried out by the CMS Collaboration [28], involving a full detector simulation and event reconstruction. These results, obtained for the benchmark point

LM5, cannot be directly translated to the case of searches for a Higgs boson with mass far below M_Z, since in the latter case the b jets resulting from the Higgs decay tend to be softer. Further phenomenological analyses of Higgs production in SUSY cascades in the MSSM with real parameters (and Higgs masses above the LEP limits) have been carried out in [29–31], with recent developments focusing on jet substructure techniques to identify highly boosted Higgs bosons and enhance the discovery significance [32, 33]. The case of a lower mass Higgs has been considered in [23], and it has been pointed out that in the CPX scenario there is a significant rate for producing a light MSSM Higgs boson in SUSY cascades, but no simulation of signal and background events was performed. The potential importance of SUSY cascades to establish a signal for a light CP-odd Higgs in the NMSSM has been pointed out in [34].

We generalize and extend the investigations carried out in [23, 34] by calculating the sparticle decay modes in a general NMSSM setting and performing a Monte Carlo simulation of the signal and the dominant background to the level of fast detector simulation. A simple cut-based analysis is performed to demonstrate that signal and background can be resolved in the $b\bar{b}$+jets channel. The observation of the Higgs decay in the $b\bar{b}$ final state would be of interest also as a direct manifestation of the Higgs Yukawa coupling.

The outline of our paper is as follows: the next section begins with a brief recapitulation of the NMSSM, presenting the scenario with a light CP-even Higgs boson in some detail. In section 3, we describe the production of squarks and gluinos at the LHC and their eventual decay into Higgs bosons through electroweak cascades involving neutralinos and charginos. Section 4 describes a phenomenological Monte Carlo analysis of these cascade processes and contains the main results of this work in terms of kinematic distributions demonstrating the separation of signal and background. The conclusions are presented in section 5.

2 The Next-to-Minimal Supersymmetric Standard Model

In this section we review briefly the elements of the NMSSM which differ from the MSSM. Our conventions for the other sectors — that remain unchanged when going to the NMSSM — follow those of [35, 36].

2.1 The Higgs sector

The Z_3-symmetric version of the NMSSM is given by the scale-invariant superpotential

$$W^{\rm NMSSM} = Y_u \hat{Q}_L \cdot H_u \hat{U}^c_L + Y_d \hat{Q}_L \cdot H_d \hat{D}^c_L + Y_e \hat{L}_L \cdot H_d \hat{E}^c_L + \lambda \hat{S} \hat{H}_u \cdot \hat{H}_d + \frac{1}{3}\kappa \hat{S}^3, \qquad (2.1)$$

where $\hat{\Phi}$ denotes a chiral superfield with scalar component Φ. The complex gauge singlet $\hat{S}$ is a new addition with respect to the MSSM. To have a complete phenomenological model the soft SUSY-breaking terms must also be specified. These are extended by couplings of the singlet field, giving new contributions to the scalar potential

$$V^{\rm NMSSM} = V^{\rm MSSM} + m_S^2 S^2 + \lambda A_\lambda S H_u \cdot H_d + \frac{1}{3}\kappa A_\kappa S^3. \qquad (2.2)$$

The NMSSM Higgs potential, which is derived from the usual F-terms, D-terms and the soft-breaking potential given by Equation (2.2), allows for a minimum where the singlet develops a vacuum expectation value (vev) $v_s = \langle S \rangle$. This induces an effective bilinear term $\lambda \langle S \rangle H_u \cdot H_d$, thus providing a dynamical explanation for the μ parameter of the MSSM in terms of $\mu_{\text{eff}} = \lambda v_s$.

Electroweak symmetry breaking (EWSB) proceeds similarly to the MSSM, and the two Higgs doublets are expanded around the potential minimum according to

$$H_d = \begin{pmatrix} v_d + \frac{1}{\sqrt{2}}(\phi_d - \mathrm{i}\sigma_d) \\ -\phi_d^- \end{pmatrix}, \qquad H_u = \begin{pmatrix} \phi_u^+ \\ v_u + \frac{1}{\sqrt{2}}(\phi_u + \mathrm{i}\sigma_u) \end{pmatrix}. \tag{2.3}$$

Equivalently, the singlet field has an expansion

$$S = v_s + \frac{1}{\sqrt{2}}(\phi_s + \mathrm{i}\sigma_s). \tag{2.4}$$

Using the minimization conditions for the potential, the scalar mass parameters $m_{H_u}^2$, $m_{H_d}^2$, and m_S^2 can be traded for

$$\begin{aligned} M_Z^2 &= g^2 v^2 = \frac{1}{2}\left(g_1^2 + g_2^2\right) v^2, \\ \tan\beta &= v_u / v_d, \\ \mu_{\text{eff}} &= \lambda v_s, \end{aligned}$$

where the doublet vevs fulfill $v^2 \equiv v_u^2 + v_d^2 = (174\ \text{GeV})^2$. Assuming a CP-invariant Higgs sector, all parameters are taken to be real. The number of parameters is increased from the MSSM. In addition to M_A (or $M_{H^\pm}$), and $\tan\beta$, the values of λ, κ, and A_κ can be chosen as free parameters.

After EWSB, the addition of a complex scalar field gives rise to additional particles in the NMSSM spectrum with respect to the MSSM: two additional Higgs bosons (one of which is CP-even, the other CP-odd) and their fermionic partner, the singlino. The elements of the tree-level mass matrix $\mathcal{M}_H^2$ for the CP-even Higgs bosons are given in the basis (ϕ_d, ϕ_u, ϕ_s) by

$$\begin{aligned} \left(\mathcal{M}_H^2\right)_{11} &= M_Z^2 \cos^2\beta + B\mu_{\text{eff}} \tan\beta, \\ \left(\mathcal{M}_H^2\right)_{22} &= M_Z^2 \sin^2\beta + B\mu_{\text{eff}} \cot\beta, \\ \left(\mathcal{M}_H^2\right)_{33} &= \frac{\lambda v^2 A_\lambda}{v_s} \cos\beta \sin\beta + \kappa v_s \left(A_\kappa + 4\kappa v_s\right), \\ \left(\mathcal{M}_H^2\right)_{12} &= \left(2\lambda^2 v^2 - M_Z^2\right) \cos\beta \sin\beta - B\mu_{\text{eff}}, \\ \left(\mathcal{M}_H^2\right)_{13} &= \lambda v \left[2\mu_{\text{eff}} \cos\beta - \left(B + \kappa v_s\right) \sin\beta\right], \\ \left(\mathcal{M}_H^2\right)_{23} &= \lambda v \left[2\mu_{\text{eff}} \sin\beta - \left(B + \kappa v_s\right) \cos\beta\right], \end{aligned} \tag{2.5}$$

where $B \equiv A_\lambda + \kappa v_s$. This matrix is diagonalized by a real 3×3 matrix with elements S_{ij}, such that the Higgs mass eigenstates H_i are given by $H_i = S_{ij}\phi_j$. For the CP-odd states,

the mass matrix elements in the basis $(\sigma_d, \sigma_u, \sigma_s)$ can be written

$$\begin{aligned}
\left(\mathcal{M}_A^2\right)_{11} &= B\mu_{\text{eff}} \tan\beta, \\
\left(\mathcal{M}_A^2\right)_{22} &= B\mu_{\text{eff}} \cot\beta, \\
\left(\mathcal{M}_A^2\right)_{33} &= \frac{\lambda v^2}{v_s} \left(B + 3\kappa v_s\right) \cos\beta \sin\beta - 3\kappa A_\kappa v_s, \\
\left(\mathcal{M}_A^2\right)_{12} &= B\mu_{\text{eff}}, \\
\left(\mathcal{M}_A^2\right)_{13} &= \lambda v \left(B - 3\kappa v_s\right) \sin\beta, \\
\left(\mathcal{M}_A^2\right)_{23} &= \lambda v \left(B - 3\kappa v_s\right) \cos\beta.
\end{aligned} \tag{2.6}$$

Similarly to the CP-even case, the massive eigenstates A_i can be written using a mixing matrix P_{ij} as $A_i = P_{ij}\sigma_j$. One degree of freedom is massless and corresponds to the neutral Goldstone boson providing the longitudinal degree of freedom to the Z boson. For some purposes it can be convenient to introduce the CP-odd mass parameter

$$M_A^2 = \frac{B\mu_{\text{eff}}}{\mathrm{c}_\beta \mathrm{s}_\beta}, \tag{2.7}$$

which corresponds to the mass of the CP-odd Higgs boson in the MSSM limit of the NMSSM.[1]

No additional charged scalar is introduced in the NMSSM, but the relation of the physical charged Higgs boson mass to the CP-odd mass parameter gets modified. At tree-level the charged Higgs mass is now given by

$$M_{H^\pm}^2 = M_A^2 + M_W^2 - \lambda^2 v^2. \tag{2.8}$$

2.2 The neutralino sector

As a result of introducing the new singlet superfield $\hat{S}$, the NMSSM comes with an additional fermion partner of the complex scalar S, the singlino. The singlino mixes with the existing four neutralinos of the MSSM. The resulting 5×5 mass matrix derives from the bilinear terms

$$\mathcal{L} = -\frac{1}{2}(\tilde{\psi}^0)^T \mathcal{M}_{\tilde{\chi}^0} \tilde{\psi}^0 + \text{h.c.}, \tag{2.9}$$

and in the basis $(-\mathrm{i}\tilde{B}, -\mathrm{i}\tilde{W}, \tilde{H}_d, \tilde{H}_u, \tilde{S})$ it is given by

$$\mathcal{M}_{\tilde{\chi}^0} = \begin{pmatrix}
M_1 & 0 & -\frac{g_1 v_d}{\sqrt{2}} & \frac{g_1 v_u}{\sqrt{2}} & 0 \\
0 & M_2 & \frac{g_2 v_d}{\sqrt{2}} & -\frac{g_2 v_u}{\sqrt{2}} & 0 \\
-\frac{g_1 v_d}{\sqrt{2}} & \frac{g_2 v_d}{\sqrt{2}} & 0 & -\mu_{\text{eff}} & -\lambda v_u \\
\frac{g_1 v_u}{\sqrt{2}} & -\frac{g_2 v_u}{\sqrt{2}} & -\mu_{\text{eff}} & 0 & -\lambda v_d \\
0 & 0 & -\lambda v_u & -\lambda v_d & 2\kappa v_s
\end{pmatrix}. \tag{2.10}$$

The upper left 4×4 submatrix is identical to the neutralino mass matrix in the MSSM. The neutralino masses can be diagonalized by a single unitary matrix N such that

$$D = \text{diag}(m_{\tilde{\chi}_i^0}) = N^* \mathcal{M}_{\tilde{\chi}^0} N^\dagger \tag{2.11}$$

[1] The MSSM limit is obtained by taking $\lambda \to 0$, $\kappa \to 0$, while keeping the ratio κ/λ and all dimensionful parameters fixed.

is real and positive with the neutralino mass eigenvalues in ascending order. Alternatively one can use a real mixing matrix N, and allow D to have negative elements. In this case the physical neutralino masses are given by $|m_{\tilde{\chi}_i^0}|$ and the neutralino couplings incorporate the additional phase shift on the neutralino fields.

2.3 The squark sector

We adopt a universal value $M_{\rm SUSY}$ for the soft SUSY-breaking scalar mass parameters. This means that, for each squark pair $\tilde{q}_L$, $\tilde{q}_R$ of a given flavour, the mass matrix attains the form

$$\mathcal{M}^2_{\tilde{q}} = \begin{pmatrix} M^2_{\rm SUSY} + m_q^2 + M_Z^2 \cos 2\beta (I_3^q - Q_q s_W^2) & m_q X_q \\ m_q X_q & M^2_{\rm SUSY} + m_q^2 + M_Z^2 \cos 2\beta Q_q s_W^2 \end{pmatrix}. \tag{2.12}$$

Here m_q is the mass of the corresponding quark, I_3^q the third component of the weak isospin, and Q_q the electric charge quantum number. For the weak mixing angle we introduce the short-hand notations $s_W \equiv \sin\theta_W$ and $c_W \equiv \cos\theta_W$. The off-diagonal elements of $\mathcal{M}^2_{\tilde{q}}$ are related to the soft trilinear couplings A_q as $X_q = A_q - \mu_{\rm eff} \cot\beta$ for up-type squarks, and $X_q = A_q - \mu_{\rm eff} \tan\beta$ for the case of down-type squarks, respectively. The mass eigenstates $(\tilde{q}_1, \tilde{q}_2)$ are obtained by a diagonalization of the mass matrix. A generic squark mass will be denoted $M_{\tilde{q}}$ below.

2.4 Scenarios with light Higgs bosons

As mentioned above, we will focus in the following on the case where the lightest CP-even Higgs boson of the NMSSM, H_1, has a mass much below M_Z. The fact that such a light Higgs, possessing a heavily suppressed coupling to gauge bosons as compared to the Higgs boson of the SM, may be unexcluded by the current search limits is known already from the case of the MSSM with complex parameters [5, 7, 8]. In the NMSSM such a situation happens more generically, in particular also for the case where the SUSY parameters are real. If the mass eigenstate H_1 has a large component of the singlet interaction state ϕ_s, its couplings to gauge bosons (and also to quarks) will be correspondingly suppressed. We will investigate the prospects for detecting such a light Higgs state through its production in SUSY cascades.

In the numerical analysis, we shall use a scenario derived from the "P4" benchmark point defined in [37]. This benchmark can be realized in models with non-universal Higgs mass parameters ($m_{H_u} \neq m_{H_d}$) at the scale of grand unification, and it is compatible with the data on the cold dark matter density. As originally defined, the P4 benchmark contains a very light CP-even Higgs boson ($M_{H_1} = 32.3$ GeV). In order to explore the full range $M_{H_1} < M_Z$, we slightly modify the scenario to allow changing the value of M_{H_1}, with the remaining phenomenology essentially unchanged. To this end we set $\lambda = 0.6$ and allow A_κ to take on values in the range 0 GeV $< A_\kappa <$ 300 GeV.[2] The soft SUSY-breaking parameters are defined directly at the SUSY-breaking scale, allowing us to consider a more

[2] The original P4 benchmark point is recovered for $\lambda = 0.53$ and $A_\kappa = 220$ GeV.

Higgs sector parameters					
λ	0.6		κ	0.12	
$\tan\beta$	2.6		μ_{eff}	-200	GeV
A_λ	-510	GeV	A_κ	0 – 300	GeV
Gaugino masses					
M_1	300	GeV	M_2	600	GeV
M_3	1000	GeV			
Trilinear couplings					
$A_t = A_b = A_\tau = 0$ GeV					
Soft scalar mass					
$M_{\text{SUSY}} = 750$ GeV, 1 TeV					

Table 1. Values for the NMSSM input parameters at the SUSY-breaking scale in the modified P4 scenario.

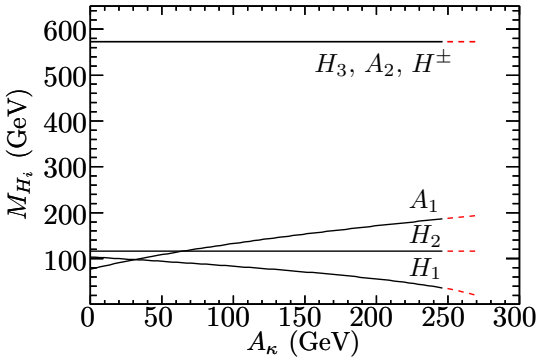

Figure 1. Higgs mass spectrum for the modified P4 scenario with $M_{\text{SUSY}} = 750$ GeV as a function of the free parameter A_κ. For $A_\kappa \gtrsim 250$ GeV (dashed) the electroweak symmetry remains unbroken in the global minimum.

general spectrum for the remaining (non-Higgs) sectors of the theory. Values for the tree-level parameters in the Higgs sector and the soft SUSY-breaking parameters in the modified P4 scenario are specified in table 1. The two values given for M_{SUSY} will be used later in the phenomenological analysis, while the values quoted in this and the next section (unless otherwise stated) have been evaluated for $M_{\text{SUSY}} = 750$ GeV.

The NMSSM Higgs masses are subject to sizable corrections beyond leading order [38–43]. In order to incorporate the most accurate predictions currently available [44], `NMSSMTools 2.3.5` [45–47] is used to compute the Higgs spectrum. The resulting Higgs masses in the modified P4 scenario are shown in figure 1 as a function of the free parameter A_κ. In the region with $A_\kappa \gtrsim 250$ GeV the global minimum of the Higgs potential does not break the electroweak symmetry; hence these values will not be considered. The masses of two Higgs bosons show a dependence on A_κ: the lightest CP-even Higgs H_1 (M_{H_1} varying from about 110 GeV to 20 GeV), and the lightest CP-odd Higgs A_1 (with M_{A_1} going from about 90 GeV to 200 GeV). H_2 is always SM-like and has a mass of about $M_{H_2} = 115$ GeV (118 GeV for $M_{\text{SUSY}} = 1$ TeV). For all Higgs masses in this

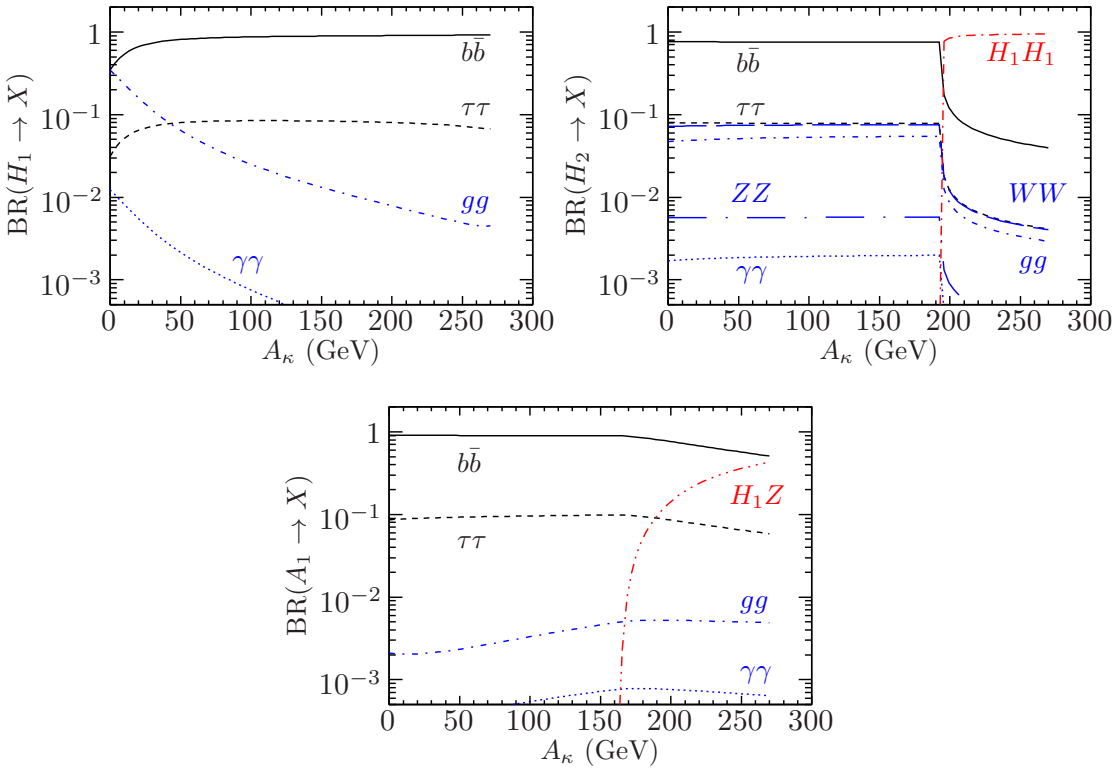

Figure 2. Branching ratios of H_1 (upper left), H_2 (upper right), and A_1 (lower) in the modified P4 scenario with $M_{\rm SUSY} = 750\,\text{GeV}$.

plot the NMSSM scenario is compatible with the direct limits from Higgs searches. The light CP-even Higgs ($M_{H_1} \ll M_Z$) is allowed due to a large singlet component, with $|S_{13}|^2$ ranging from 0.9 for $A_\kappa = 0$ GeV to $|S_{13}|^2 > 0.99$ for $A_\kappa = 250$ GeV. As a consequence, the couplings of H_1 to vector bosons are heavily suppressed, so that the cross section for production through Higgsstrahlung drops below the LEP limit. The pair production of A_1H_1 is even further suppressed by the large singlet fractions of both H_1 and A_1, while production of H_2A_1 and H_2Z are beyond the kinematic reach of LEP. The full mass ranges shown in the figure are also compatible with the constraints from B-physics implemented in `NMSSMTools 2.3.5` [45–47], as expected when the charged Higgs boson is heavy [48, 49]. The precise values obtained here for the heavy Higgs masses are $M_{H^\pm} \simeq 563$ GeV, and $M_{H_3} \simeq M_{A_2} \simeq 572$ GeV. None of the heavy Higgs bosons will play any role in the following. With the negative sign for the effective μ parameter, this model cannot be used to explain the observed deviation in the anomalous magnetic moment of the muon (see e.g. [50] for a review). However — since the considered value of $\tan\beta$ is rather low — the predicted value for $(g-2)_\mu$ at least stays close to that in the SM.

The branching ratios of the three lightest Higgs states, H_1, H_2, and A_1, are given in figure 2. As can be seen from this figure, the light singlet H_1 decays preferentially into $b\bar{b}$, with $\text{BR}(H_1 \to b\bar{b}) \simeq 90\%$ over the full mass range. The subdominant decay into $\tau\tau$ basically saturates the H_1 width. For lower values of A_κ — where $M_{H_1} \gtrsim 90$ GeV — we note a similar enhancement of $\text{BR}(H_1 \to \gamma\gamma)$ compared to a SM Higgs with the

same mass as recently discussed in [51]. The H_2 has a more complicated decay pattern, in particular for low A_κ where $H_2 \to b\bar{b}$ dominates and several competing modes ($H_2 \to \tau\tau$, gg, WW) each have a branching fraction around 10%. In this region H_2 is SM-like, and the same search strategies as devised for the SM Higgs (and the lightest MSSM Higgs boson in the decoupling limit) should apply. This situation changes radically when the channel $H_2 \to H_1 H_1$ opens. When this is the case, the $H_2 \to H_1 H_1$ mode becomes completely dominant. Finally, the lightest CP-odd Higgs A_1 decays predominantly into $b\bar{b}$, with a large fraction going into the mode $A_1 \to H_1 Z$ when kinematically accessible.

In the neutralino sector the mass spectrum is independent of A_κ (and $M_{\rm SUSY}$) at lowest order, cf. equation (2.10), and therefore remains fixed at:

$$M_{\tilde{\chi}_1^0} = 97.6 \text{ GeV}, \quad M_{\tilde{\chi}_2^0} = 227 \text{ GeV}, \quad M_{\tilde{\chi}_3^0} = 228 \text{ GeV}$$
$$M_{\tilde{\chi}_4^0} = 304 \text{ GeV}, \quad M_{\tilde{\chi}_5^0} = 616 \text{ GeV}.$$

There is a clear hierarchy in the mass parameters, which leads to a small mixing between the neutralinos. The heaviest neutralino is almost exclusively wino, and $\tilde{\chi}_4^0$ is mostly bino. The intermediate mass states $\tilde{\chi}_2^0$, and $\tilde{\chi}_3^0$ are predominantly Higgsino, while the lightest neutralino $\tilde{\chi}_1^0$ is the singlino. The lightest neutralino is also the overall lightest supersymmetric particle (LSP) in these scenarios and thereby a candidate for cold dark matter.

3 Higgs production in the light H_1 scenario

3.1 Standard channels

The rate for direct production of a light singlet H_1 in gluon fusion, $gg \to H_1$, is proportional to its reduced (squared) coupling to quarks. Compared to a SM Higgs boson with the same mass, the dominant top loop contribution contains the additional factor $|S_{12}|^2/\sin^2\beta$. The size of $|S_{12}|^2$ is limited from above by $|S_{12}|^2 \leq 1-|S_{13}|^2$, where S_{13} is the singlet component. For $M_{H_1} \ll M_Z$, where $|S_{13}| \to 1$, the rate for this process gets heavily suppressed. The cross section for H_1 in weak boson fusion, involving the coupling of H_1 to gauge bosons, is similarly suppressed. In scenarios where $M_{H_1} > M_Z$ (corresponding to the mass range below the LEP limit on a SM-like Higgs which is unexcluded in the MSSM with real parameters) the suppression of $gg \to H_1$ can be overcome by an increased branching ratio for $H_1 \to \gamma\gamma$ [51].

For $A_\kappa \gtrsim 200$ GeV in the modified P4 scenario, H_1 is light enough to be produced through the decay of the SM-like $H_2 \to H_1 H_1$, which can be dominant, see figure 2. The production of H_2 in standard channels is not suppressed. The resulting two-step decay chain leads to "unusual" final states for H_2: $4b$ (about 82% of all decays), $2b2\tau$ (17%), and 4τ (0.6%). These final states make it difficult to establish a Higgs signal, as it has been demonstrated, for instance, by the numerous attempts [52–56] to establish a "no-loose" theorem for NMSSM Higgs searches when decays of the SM-like Higgs into lighter Higgses are open.

Another possibility to produce H_1 in Higgs decays would be through the decay $A_1 \to H_1 Z$. However, the singlet nature of A_1 in the modified P4 scenario leads to a suppression of A_1 production similar to that for H_1, and this mode is therefore not likely to be accessible.

The direct production of the heavy Higgs bosons H_3, A_2, and $H^\pm$ is in principle not suppressed with respect to the MSSM case, but at a mass close to 600 GeV and low $\tan\beta$ the observation of those states at the LHC will be difficult even at high luminosity. A large fraction of the heavy Higgs bosons in this scenario will decay into lighter Higgs bosons, neutralinos and charginos. A detailed investigation of these channels could possibly be of interest for a study assuming a very high luminosity at 14 TeV, but is beyond the scope of the present paper.

In summary, it will be problematic to produce and reconstruct the light H_1 in any of the standard channels proposed for Higgs production at the LHC. We shall focus instead on the possibility to produce H_1 in the decays of supersymmetric particles.

3.2 SUSY cascades

As discussed in the previous section, inclusive production of the heavier state H_2 with subsequent decay $H_2 \to H_1 H_1$ may be difficult to observe at the LHC. However, the related process where a heavier neutralino decays into a lighter neutralino and a Higgs boson (and the corresponding mode of the decay of the heavier chargino) may offer better prospects. In fact, a light Higgs boson in the mass range below M_Z may occur in a large fraction of cascade decays of heavier SUSY particles that are produced via strong interaction processes. The hard scale associated with the sparticle production can lead to event signatures which are more clearly separable from the SM backgrounds than those of inclusive Higgs production followed by a decay into a pair of H_1 states. The processes of interest are

$$\tilde{\chi}_i^0 \to \tilde{\chi}_j^0 H_k, \quad \tilde{\chi}_i^0 \to \tilde{\chi}_j^0 A_k, \tag{3.1}$$

$$\tilde{\chi}_2^\pm \to \tilde{\chi}_1^\pm H_k, \quad \tilde{\chi}_2^\pm \to \tilde{\chi}_1^\pm A_k, \tag{3.2}$$

where H_k (A_k) denotes any of the CP-even (CP-odd) Higgs bosons. As mentioned above we do not consider scenarios where the heavier $H^\pm$ is produced in the cascades. The partial width for the neutralino decay (3.1) is given at tree-level by

$$\Gamma(\tilde{\chi}_i^0 \to \tilde{\chi}_j^0 H_k) = \frac{|\mathcal{S}_{ijk}|^2}{16\pi m_{\tilde{\chi}_i^0}^3} \tau^{1/2}(m_{\tilde{\chi}_i^0}^2, m_{\tilde{\chi}_j^0}^2, m_{H_k}^2) \left(m_{\tilde{\chi}_i^0}^2 + m_{\tilde{\chi}_j^0}^2 - m_{H_k}^2 + 2 m_{\tilde{\chi}_i^0} m_{\tilde{\chi}_j^0} \right), \tag{3.3}$$

with a CP-even Higgs in the final state and

$$\Gamma(\tilde{\chi}_i^0 \to \tilde{\chi}_j^0 A_k) = \frac{|\mathcal{P}_{ijk}|^2}{16\pi m_{\tilde{\chi}_i^0}^3} \tau^{1/2}(m_{\tilde{\chi}_i^0}^2, m_{\tilde{\chi}_j^0}^2, m_{A_k}^2) \left(m_{\tilde{\chi}_i^0}^2 + m_{\tilde{\chi}_j^0}^2 - m_{A_k}^2 - 2 m_{\tilde{\chi}_i^0} m_{\tilde{\chi}_j^0} \right) \tag{3.4}$$

for the decay into a CP-odd scalar. The Källén function $\tau(x,y,z) = (x-y-z)^2 - 4yz$, and the coupling factors are

$$\begin{aligned} \mathcal{S}_{ijk} =& \frac{e}{2 c_W s_W} \Big[(S_{k1} N_{i3} - S_{k2} N_{i4}) (c_W N_{j2} - s_W N_{j1}) \Big] - \\ & \frac{\lambda}{\sqrt{2}} \Big[N_{i5} (S_{k1} N_{j4} + S_{k2} N_{j3}) + S_{k3} N_{i4} N_{j3} \Big] + \frac{\kappa}{\sqrt{2}} S_{k3} N_{i5} N_{j5} + i \leftrightarrow j, \end{aligned} \tag{3.5}$$

and

$$
\begin{aligned}
-\mathrm{i}\mathcal{P}_{ijk} =& \frac{e}{2c_W s_W}\Big[(P_{k1}N_{i3} - P_{k2}N_{i4})\,(c_W N_{j2} - s_W N_{j1})\Big] + \\
& \frac{\lambda}{\sqrt{2}}\Big[N_{i5}\,(P_{k1}N_{j4} + P_{k2}N_{j3}) + P_{k3}N_{i4}N_{j3}\Big] - \frac{\kappa}{\sqrt{2}}P_{k3}N_{i5}N_{j5} + i \leftrightarrow j,
\end{aligned}
\tag{3.6}
$$

where the mixing matrices S_{ij}, P_{ij}, and N_{ij} are defined in section 2.1. Equations (3.3)–(3.6) assume a real neutralino mixing matrix N_{ij} and signed neutralino masses. Competing neutralino decay modes are into vector bosons, $\tilde{\chi}_i^0 \to \tilde{\chi}_j^0 Z$ and $\tilde{\chi}_i^0 \to \tilde{\chi}_j^\pm W^\mp$. For brevity we refrain from giving expressions for these (and the corresponding chargino decay modes) here; they can be found in [57]. A detailed analysis of the $W^\pm$ mode is performed in [58]. Since the squarks and sleptons are assumed to be heavy, there are no open two-body decay modes of the neutralinos into the sfermion sector. Also slepton-mediated three-body decays — which can dominate over the two-body decays in certain scenarios — are numerically irrelevant for the same reason.

The branching fractions for the relevant decay channels have been computed at leading order using `FeynArts`/`FormCalc` [59, 60] and a purpose-built Fortran code.[3] Results for the neutralino branching ratios in the modified P4 scenario are shown in figure 3. The decay modes of $\tilde{\chi}_2^0$ and $\tilde{\chi}_3^0$ (upper row of figure 3) — which are both Higgsino-like — show similar patterns for large values of A_κ. The dominant mode is always $\tilde{\chi}_i^0 \to \tilde{\chi}_1^0 Z$ with a branching ratio of about 50%, but the Higgs channels are also significant with $\mathrm{BR}(\tilde{\chi}_i^0 \to \tilde{\chi}_1^0 H_1) \gtrsim 0.3$ and $\mathrm{BR}(\tilde{\chi}_i^0 \to \tilde{\chi}_1^0 H_2) \sim 0.15$. An important point to note here is that the branching ratios of $\tilde{\chi}_2^0$ and $\tilde{\chi}_3^0$ are quite insensitive to changes in M_{H_1} (A_κ). For the heavier neutralinos, $\tilde{\chi}_4^0$ and $\tilde{\chi}_5^0$ (lower row of figure 3), which also carry a larger gaugino fraction, the decay pattern is more complicated. Of largest interest for Higgs production is the sizable rate for $\tilde{\chi}_4^0 \to \tilde{\chi}_3^0 H_1$ (once A_κ is sufficiently large to make this decay mode kinematically possible), and the fact that direct decays of $\tilde{\chi}_5^0$ to the LSP are suppressed. This will lead to neutralino decay chains with intermediate (Higgsino) steps. Everything taken together, we can expect a large number of light Higgs bosons to be produced in neutralino cascade decays.

The light chargino $\tilde{\chi}_1^\pm$ decays exclusively into the LSP and a W boson, while the corresponding decay channels for the heavier chargino $\chi_2^\pm$ are shown in figure 4. Even if the dominant mode is $\tilde{\chi}_2^\pm \to \tilde{\chi}_1^\pm W^\mp$, independently of A_κ, there are several channels with a branching fraction of order 20% of interest for Higgs production. These include the mode $\tilde{\chi}_2^\pm \to \tilde{\chi}_1^\pm H_2$ and the decays into intermediate-mass Higgsinos, $\tilde{\chi}_2^\pm \to \tilde{\chi}_{2,3}^0 W^\pm$.

The heavier neutralinos and the heavy chargino, from which a Higgs could emerge as decay product, can either be produced at the LHC directly or in the decay of a heavier SUSY particle. The cross section for direct production of neutralino pairs is small, only $\mathcal{O}(\mathrm{fb})$ at $\sqrt{s} = 14$ TeV, and the reach in these channels will be rather limited even for high luminosity. The large cross sections for production of strongly interacting sparticles (squarks and gluinos), on the other hand, are potentially more promising as a source of the heavier neutralino states and the heavier chargino. Exploiting cascade decays of this kind

[3] A `FeynArts` model file for the NMSSM has been obtained using `FeynRules` [61] and `SARAH` [62]. Details on this implementation will be presented elsewhere.

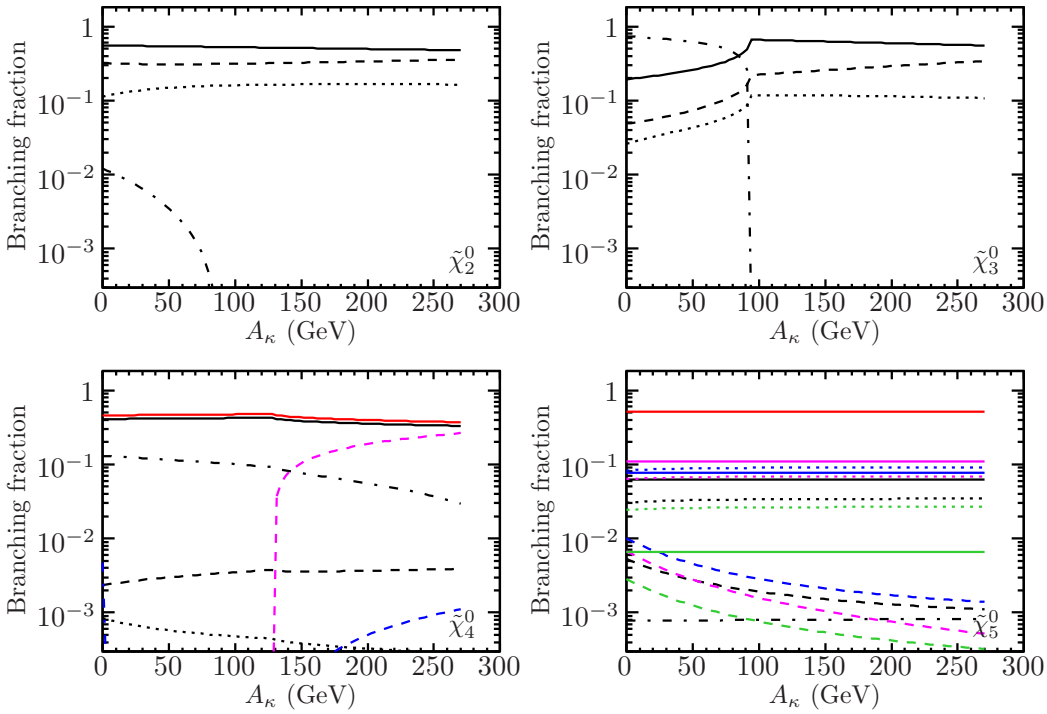

Figure 3. Branching ratios in the modified P4 scenario for $\tilde{\chi}_i^0 \to \tilde{\chi}_j^0 Z$ (solid), $\tilde{\chi}_i^0 \to \tilde{\chi}_j^0 H_1$ (dashed), $\tilde{\chi}_i^0 \to \tilde{\chi}_j^0 H_2$ (dotted), and $\tilde{\chi}_i^0 \to \tilde{\chi}_j^0 A_1$ (dot-dashed). The color coding indicates the final state neutralino $j = 1$ (black), $j = 2$ (blue), $j = 3$ (magenta), $j = 4$ (green), or the chargino mode $\tilde{\chi}_i^0 \to \tilde{\chi}_1^\pm W^\mp$ (red).

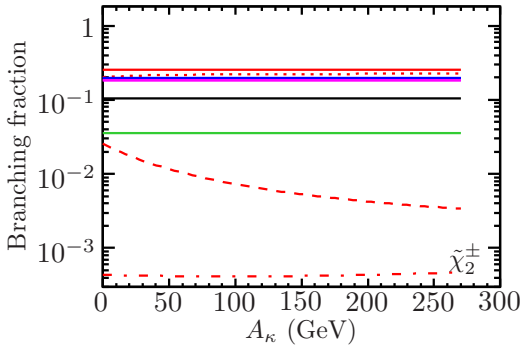

Figure 4. Branching ratios of $\tilde{\chi}_2^\pm$ in the modified P4 scenario. Neutralino final states $\tilde{\chi}_2^\pm \to \tilde{\chi}_i^0 W^\pm$ (solid) are shown with the same color coding as for figure 3. Modes with a final state $\tilde{\chi}_1^\pm$ are shown in red: $\tilde{\chi}_2^\pm \to \tilde{\chi}_1^\pm Z$ (solid), $\tilde{\chi}_2^\pm \to \tilde{\chi}_1^\pm H_1$ (dashed), $\tilde{\chi}_2^\pm \to \tilde{\chi}_1^\pm H_2$ (dotted), $\tilde{\chi}_2^\pm \to \tilde{\chi}_1^\pm A_1$ (dot-dashed).

furthermore has the advantage that additional high-p_T jets are produced, which facilitates triggering and event selection.

We use `Prospino` to calculate the NLO cross sections for production of $pp \to \tilde{g}\tilde{g}$, $pp \to \tilde{q}\tilde{q}$, $pp \to \tilde{q}\bar{\tilde{q}}$, and $pp \to \tilde{g}\tilde{q}$ according to [63], with CTEQ6 [64] parton distributions and a common choice of renormalization and factorization scales as the average mass of the final state (SUSY) particles. Numerical results are given in table 2 for the two centre-of-

Masses (GeV)		$\sigma_{\rm LO}$ (pb)					$\sigma_{\rm NLO}$ (pb)				
$M_{\tilde{g}}$	$M_{\tilde{q}}$	$\tilde{g}\tilde{g}$	$\tilde{q}\tilde{q}$	$\tilde{g}\tilde{q}$	$\tilde{q}\bar{\tilde{q}}$	Σ	$\tilde{g}\tilde{g}$	$\tilde{q}\tilde{q}$	$\tilde{g}\tilde{q}$	$\tilde{q}\bar{\tilde{q}}$	Σ
$\sqrt{s} = 7$ TeV											
750	750	0.03	0.23	0.25	0.05	0.56	0.07	0.27	0.39	0.08	0.82
1000	750	0.002	0.19	0.06	0.05	0.31	0.006	0.21	0.10	0.07	0.39
1000	1000	0.001	0.03	0.02	0.004	0.06	0.005	0.04	0.04	0.006	0.08
$\sqrt{s} = 14$ TeV											
750	750	1.18	1.67	5.20	1.06	9.11	2.21	2.06	6.78	1.53	12.6
1000	750	0.15	1.41	1.86	0.96	4.38	0.32	1.59	2.44	1.34	5.69
1000	1000	0.14	0.42	0.87	0.18	1.61	0.31	0.51	1.19	0.26	2.27
1500	1500	0.01	0.04	0.05	0.01	0.10	0.01	0.05	0.07	0.02	0.15

Table 2. Total production cross sections for $pp \to \tilde{g}\tilde{g}$, $pp \to \tilde{q}\tilde{q}$, $pp \to \tilde{g}\tilde{q}$, and $pp \to \tilde{q}\bar{\tilde{q}}$ at LO and NLO SUSY-QCD from `Prospino`. The squark cross sections are summed over the four "light" squark flavours. No kinematic cuts have been applied here.

mass energies 7 TeV and 14 TeV. The cross sections for $pp \to \tilde{t}\bar{\tilde{t}}$ and $pp \to \tilde{b}\bar{\tilde{b}}$ [65] are also calculated and included in the analysis, but since they turn out to be significantly smaller than $\sigma(pp \to \tilde{q}\bar{\tilde{q}})$ they are not shown in the table. In order to give some indication of the expected change in the number of events for different scenarios, the results are presented for several values of the squark masses, $M_{\tilde{q}}$, and the gluino mass, $M_{\tilde{g}}$. The mass ranges are selected to respect the published limits from ATLAS [66–70] and CMS [71–74] based on the 2010 data. Taking into account also the most recent results [75, 76], the $M_{\tilde{q}} = 750$ GeV case appears to be under some pressure. We present the results of our analysis below for the two cases $M_{\rm SUSY} = 750$ GeV and $M_{\rm SUSY} = 1$ TeV (the leading order squark masses are obtained from $M_{\rm SUSY}$ through eq. (2.12), to which higher order corrections are then added).

The nearly mass-degenerate squarks decay preferentially into the SUSY-EW sector. Direct decays into Higgs bosons (or Higgsinos) are negligible for squarks of the first two generations due to the small Yukawa couplings. In contrast to the MSSM, the neutralinos also have a singlino component to which no squark couples. The left-handed squarks decay mainly into the wino, $\tilde{q}_L \to \tilde{W}^0 q$, $\tilde{q}_L \to \tilde{W}^\pm q'$, while the right-handed squarks decay mostly to the bino, $\tilde{q}_R \to \tilde{B} q$. Numerically, this leads to squark decay modes listed in table 3 for the case with a soft scalar mass of $M_{\rm SUSY} = 750$ GeV. The squark decay pattern for $M_{\rm SUSY} = 1$ TeV is qualitatively similar.[4] Since the gaugino components are largest in the two heaviest neutralinos, the neutralinos produced in the squark decays tend to give rise to cascade decays with several steps.

Finally, we note that the gluinos decay 'democratically' through $\tilde{g} \to \tilde{q}\bar{q}$ into all flavours, with rates governed only by the available phase space.

[4] The main numerical difference is an increase of $\mathrm{BR}(\tilde{u}_L \to q' \tilde{\chi}_2^\pm)$ to 60% at the expense of a reduced $\mathrm{BR}(\tilde{u}_L \to q' \tilde{\chi}_1^\pm) = 3.9 \times 10^{-2}$.

Final state	$\tilde{u}_L$	$\tilde{u}_R$	$\tilde{d}_L$	$\tilde{d}_R$
$\tilde{q} \to q\tilde{\chi}_1^0$	2.9×10^{-3}	2.6×10^{-3}	6.3×10^{-3}	2.6×10^{-3}
$\tilde{q} \to q\tilde{\chi}_2^0$	8.1×10^{-3}	5.4×10^{-3}	1.6×10^{-2}	5.4×10^{-3}
$\tilde{q} \to q\tilde{\chi}_3^0$	1.9×10^{-3}	4.5×10^{-2}	2.0×10^{-2}	4.6×10^{-2}
$\tilde{q} \to q\tilde{\chi}_4^0$	6.6×10^{-2}	0.95	2.9×10^{-2}	0.95
$\tilde{q} \to q\tilde{\chi}_5^0$	0.29	–	0.32	–
$\tilde{q} \to q'\tilde{\chi}_1^\pm$	9.6×10^{-2}	–	3.3×10^{-4}	–
$\tilde{q} \to q'\tilde{\chi}_2^\pm$	0.54	–	0.61	–

Table 3. Branching ratios for the first and second generation squarks into neutralinos and charginos in the modified P4 scenario with $M_{\rm SUSY} = 750$ GeV. Results for channels with a branching ratio below 10^{-4} are not shown.

4 LHC analysis

In order to assess whether the process discussed in the previous section can be useful as a Higgs search channel at the LHC we perform a Monte Carlo simulation. Here we use as benchmark the modified P4 scenario with the two different settings for the soft scalar mass: $M_{\rm SUSY} = 750$ GeV and $M_{\rm SUSY} = 1$ TeV. The $\overline{\rm DR}$ value of the gluino mass parameter is set to $M_3 = 1$ TeV. We select A_κ such that $M_{H_1} \simeq 40$ GeV, which also affects M_{H_2}, M_{A_1} and the branching ratios in the two cases as discussed in section 3. We have chosen this value of M_{H_1} as an illustrative example of our scenario with 20 GeV $< M_{H_1} < M_Z$ and in order to make contact with the analyses of the "CPX hole" in the MSSM with complex parameters. Our results however depend only very mildly on the specific choice for M_{H_1}. The simulation results are presented below both for LHC running at centre-of-mass energies of 7 TeV and 14 TeV.

The squark and gluino-induced cascades in general give rise to a final state with high multiplicities and several hard jets, as well as large missing transverse momentum due to the presence of the LSP at the end of each decay chain. The minimal signal cascades (defined to be those with at least one Higgs boson present) generated by the production of a single squark or gluino correspond to

$$\tilde{q} \to q\tilde{\chi}_i^0 \to q\tilde{\chi}_1^0 H_k \to q\tilde{\chi}_1^0 b\bar{b}, \qquad n_j \geq 1, \quad n_b \geq 2, \tag{14 a}$$

$$\tilde{g} \to g\tilde{q} \to gq\tilde{\chi}_i^0 \to gq\tilde{\chi}_1^0 H_k \to gq\tilde{\chi}_1^0 b\bar{b}, \qquad n_j \geq 2, \quad n_b \geq 2. \tag{14 b}$$

Equations (14 a) and (14 b) show the minimum number of light and heavy flavour (b-) jets expected in the signal. Each event contains production of a pair of sparticles and their associated jets, meaning that the full signature for production of at least one H_1 in the hadronic final state will be $n_j \geq 2$, $n_b \geq 2$. Since direct decays of the heavier (mainly gaugino) neutralinos into the singlino LSP are practically absent (cf. figure 3), most signal cascades will contain an intermediate Higgsino step which will add further particles in the final state. The typical jet multiplicity will also be higher due to additional QCD activity, in particular for gluon-initiated processes.

4.1 Event Generation

For the event generation, we use `MadGraph/MadEvent 4.4.44` [77] to calculate the leading order matrix elements for $pp \to \tilde{g}\tilde{g}, \tilde{q}\tilde{q}, \tilde{g}\tilde{q}, \tilde{q}\bar{\tilde{q}}, t\bar{\tilde{t}}$, and $\tilde{b}\bar{\tilde{b}}$. The different event categories are weighted by the corresponding NLO cross sections to produce an inclusive SUSY sample. The resonance decay chains are then generated with `PYTHIA 6.4` [78] using the NMSSM decay rates calculated above as input through the SUSY Les Houches accord [36]. The `PYTHIA` generator is also used to produce additional QCD radiation through initial- and final state parton showers, for parton fragmentation, and to generate multiple interactions for the underlying event. This produces fully dressed hadronic events which are passed through the fast simulation of the ATLAS detector performance implemented in the `Delphes` package [79].[5] Hadronic jets are clustered using the anti-k_T algorithm [80] with a jet radius measure of $R = 0.4$.

Since for the lightest Higgs boson the decay to $b\bar{b}$ is favored, the probability η_b to correctly identify jets originating from bottom partons (b-tagging efficiency) becomes a crucial quantity for the analysis. Based on [81] we parametrize this efficiency as a constant $\eta_b = 0.6$ with respect to both the detector geometry and the jet energy scale. Only jets in the central tracking region $|\eta| < 2.5$ can be tagged. The rate for misidentification as a b-jet is assumed to be $\eta_c = 0.1$ for charm jets, and $\eta_q = 0.01$ for jets produced by light quarks and gluons. The actual tagging algorithm implemented in the `Delphes` simulation is not based on a particular experimental method to identify b-jets. The algorithm determines if a jet is close enough in ΔR to a "true" b parton. When this is the case, the efficiencies given above are applied to determine if the tagging is successful or not.

4.2 Backgrounds

Based on the event signature, SM production of $t\bar{t}$ with at least one hadronically decaying W boson (or additional jet activity) constitutes an irreducible background to the Higgs signal. We can *a priori* expect this to be the most important SM background since the scale for the SUSY-QCD processes is high (> 1 TeV). In principle there are other sources of background from production of $W+$jets ($b\bar{b}$), $Z+$jets ($b\bar{b}$), direct production of $b\bar{b}+$jets, or from QCD multijets. The cross sections for these processes are large compared to the signal cross section, with QCD multijets the largest and thereby potentially the most serious. However, for QCD jet production to constitute a background to the Higgs signal simultaneously a double misidentification of heavy flavour jets and a large mismeasurement of the missing transverse energy is required. It is furthermore difficult to simulate this background reliably, since extreme kinematical fluctuations — or experimental effects — would be necessary to produce the signal-like events. A detailed study of the experimental effects would require a full detector simulation, which is beyond the scope of the present paper. However, the dominance of the $t\bar{t}$ background over other SM processes, such as $W+$jets or $Z+$jets, for our final state has also been demonstrated experimentally by the results from SUSY searches with b-jets and missing E_T [68]. We therefore proceed under

[5] Running the same `Delphes` analysis with the "CMS" detector setup and similar parameters for jets and heavy flavour tagging, no significant differences are observed in the output.

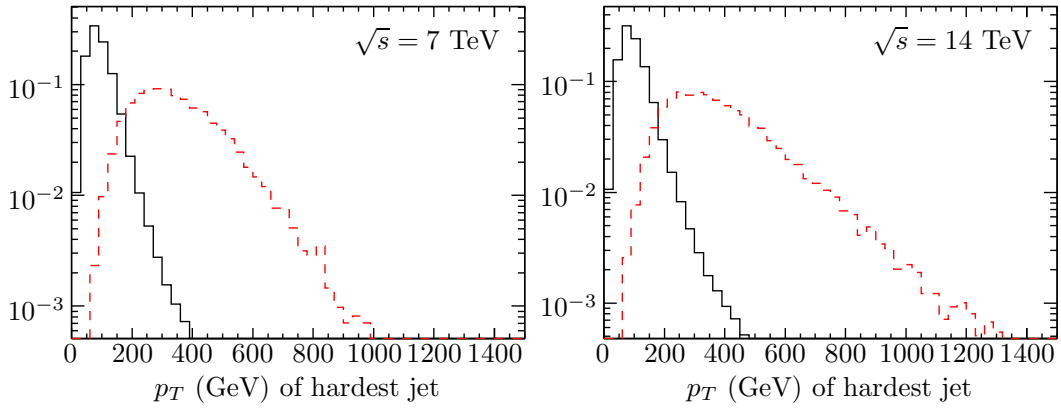

Figure 5. Transverse momentum distribution of the hardest (non-b) jet at 7 TeV (left) and 14 TeV (right) for the inclusive SUSY sample with $M_{\rm SUSY} = 750$ GeV(dashed) and SM $t\bar{t}$ background (solid). The histograms are normalized to unity.

the assumption that the cuts devised to suppress the irreducible $t\bar{t}$ background will also be efficient for suppressing the other SM backgrounds as well.

For the normalization of the $t\bar{t}$ background we use the NLO cross section $\sigma(pp \to t\bar{t}) = 902\,\text{pb}$ ($\sqrt{s} = 14$ TeV) and $\sigma(pp \to t\bar{t}) = 162\,\text{pb}$ ($\sqrt{s} = 7$ TeV), computed with the `HATHOR` package [82] for $m_t = 173.3$ GeV and MSTW2008 PDFs [83]. In this way a consistent NLO normalization is used for both the signal and background events. The $t\bar{t}$ background is generated in the same Monte Carlo framework as already described for the signal.

In addition to the SM backgrounds, the process we are interested in receives an important background from the SUSY cascade itself. Any final state containing two b-jets which do not result from an intermediate Higgs boson contributes to this background. Attempting to suppress the SUSY background events would require additional cuts that depend on the kinematics of the decay chains. This is something which may indeed be possible to devise once information on the supersymmetric spectrum has become available, but since we do not want to make any particular assumptions on the pattern of the SUSY spectrum, no selection will be applied aiming to reduce the SUSY background. Instead we will consider the inclusive $b\bar{b}$ mass spectrum directly after applying the cuts designed to reduce the SM background to determine if a Higgs signal can be extracted.

4.3 Event Selection

As a first step, we perform a preselection of the expected event topology, demanding $n_j \geq 2$, $n_b \geq 2$. All reconstructed jets are required to have a minimum $p_T \geq 25$ GeV.

Figure 5 shows the p_T distribution for the hardest jet in each event, comparing the inclusive SUSY events (with $M_{\rm SUSY} = 750$ GeV) to the $t\bar{t}$ background. We show the results for the two cases $\sqrt{s} = 7$ TeV (left) and $\sqrt{s} = 14$ TeV (right). In order to illustrate the effect of applying cuts to this variable, each histogram is normalized to unity. From figure 5 it is clear that the leading jet from the SUSY events has a much harder scale compared to the $t\bar{t}$ events. This can be understood as a result of the large boost obtained by the light

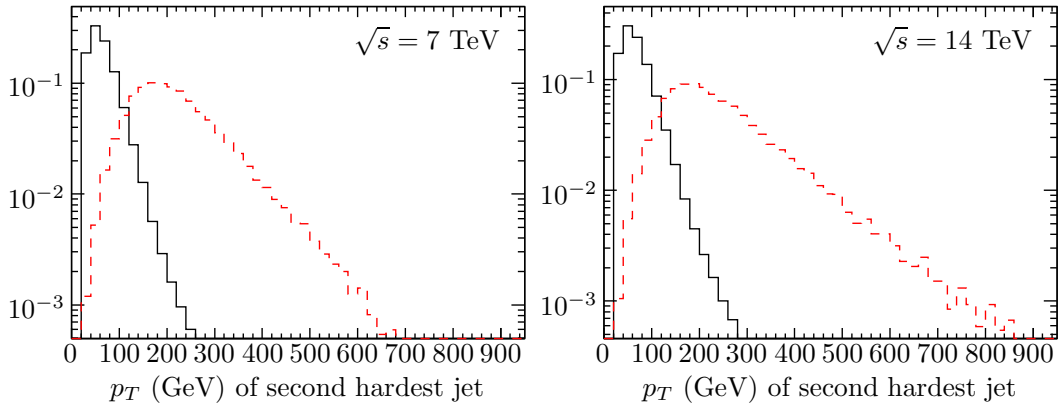

Figure 6. Transverse momentum distribution of the second hardest jet at 7 TeV (left) and 14 TeV (right) for the inclusive SUSY sample with $M_{\mathrm{SUSY}} = 750$ GeV (dashed) and SM $t\bar{t}$ background (solid). The histograms are normalized to unity.

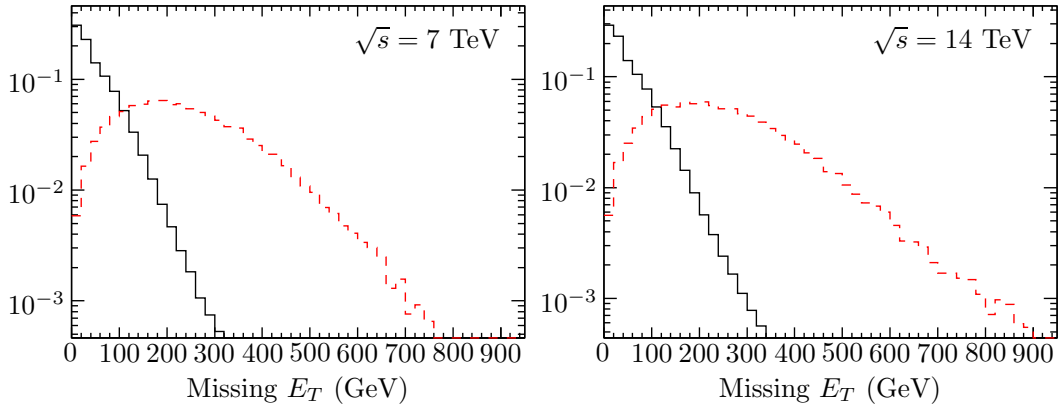

Figure 7. Missing transverse energy at 7 TeV (left) and 14 TeV (right) for the inclusive SUSY sample (dashed) and SM $t\bar{t}$ background (solid). The histograms are normalized to unity.

quark jets originating from squark decays. It can also be seen that there is only a minor scaling difference in the jet p_T distribution between the 7 TeV and 14 TeV cases. The same is true for the second hardest (light) jet, for which the corresponding p_T distribution is shown in figure 6. Similar differences between signal and background can be observed also for the third and fourth jet when they are present.

With each cascade ending in the stable LSP, a large missing transverse energy $\not{E}_T$ is expected for the signal events. This distribution is displayed in figure 7, and shows indeed that the SUSY distribution peaks at high $\not{E}_T$ values ($\gtrsim 200$ GeV). This is therefore an important discriminating variable to suppress the background from $t\bar{t}$ events, where the missing transverse energy is due to neutrinos from leptonic W decays. As already mentioned, a hard cut on $\not{E}_T$ is also necessary to suppress the background from ordinary QCD multijet events and direct production of $b\bar{b}$. A further advantage of the large $\not{E}_T$ is that it can be used for triggering.

The final kinematical distribution we are going to consider is displayed in figure 8. It

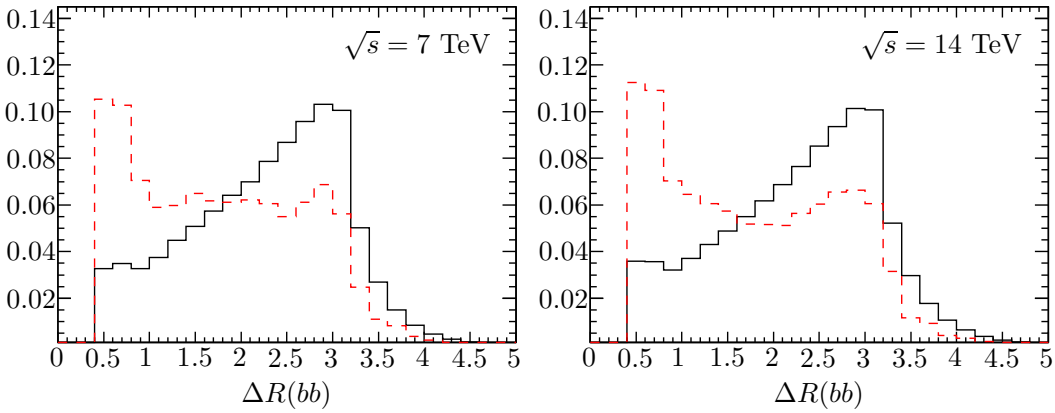

Figure 8. Distribution in $\Delta R(b\bar{b})$ at 7 TeV (left) and 14 TeV (right) for the inclusive SUSY sample (dashed) and SM $t\bar{t}$ background (solid). The histograms are normalized to unity. In events containing more than two b-jets, all possible combinations have been included.

$M_{\rm SUSY} = 750$ GeV	Incl. SUSY	Signal	Background
Generated events	18 465	8 261	10 195
$n_j \geq 2$, $n_b \geq 2$	4 048	2 786	1 262
$p_T^{\rm jet\,1} > 250$ GeV, $p_T^{\rm jet\,2} > 100$ GeV	2 436	1 738	698
$\not{E}_T > 150$ GeV	1 735	1 211	524
$\min\left[\Delta R(bb)\right] < 1.5$	1 014	774	240
Total efficiency	5.5×10^{-2}	9.4×10^{-2}	2.4×10^{-2}

$M_{\rm SUSY} = 1$ TeV	Incl. SUSY	Signal	Background
Generated events	20 671	10 923	9 748
$n_j \geq 2$, $n_b \geq 2$	5 313	4 344	969
$p_T^{\rm jet\,1} > 250$ GeV, $p_T^{\rm jet\,2} > 100$ GeV	4 642	3 828	814
$\not{E}_T > 150$ GeV	3 705	3 036	669
$\min\left[\Delta R(bb)\right] < 1.5$	2 544	2 170	374
Total efficiency	0.12	0.20	3.8×10^{-2}

Table 4. Number of events remaining after each step of the event selection at $\sqrt{s} = 7$ TeV. The SUSY events are classified as signal or background based on the presence of (at least one) Higgs boson in the decay chain. The total number of generated events in the inclusive sample is arbitrary.

shows the separation in $\Delta R = \sqrt{(\Delta\eta)^2 + (\Delta\phi)^2}$ between pairs of b-jets. For events with $n_b > 2$ all possible combinations have been included. The signal distribution is seen to peak near the minimum separation of $\Delta R = 0.4$ set by the jet measure, while the $t\bar{t}$ background prefers the b-jets to be more back-to-back and peaks at $\Delta R \sim \pi$.

The precise cuts applied — and their effect on the event selection — are shown for the SUSY events in table 4 (for the 7 TeV case) and table 5 (14 TeV). Table 6 gives the corresponding information for the SM $t\bar{t}$ background. Note that the number of generated events in these tables does not correspond to any particular luminosity, but is rather

$M_{\mathrm{SUSY}} = 750$ GeV	Incl. SUSY	Signal	Background
Generated events	23 771	10 874	12 897
$n_j \geq 2$, $n_b \geq 2$	5 009	3 610	1 399
$p_T^{\mathrm{jet}\,1} > 250$ GeV, $p_T^{\mathrm{jet}2} > 100$ GeV	3 287	2 422	865
$\not{E}_T > 200$ GeV	1 935	1 400	535
$\min\left[\Delta R(bb)\right] < 1.2$	991	775	216
Total efficiency	4.2×10^{-2}	7.1×10^{-2}	1.7×10^{-2}

$M_{\mathrm{SUSY}} = 1$ TeV	Incl. SUSY	Signal	Background
Generated events	20 232	10 557	9 675
$n_j \geq 2$, $n_b \geq 2$	5 428	4 338	1 090
$p_T^{\mathrm{jet}\,1} > 250$ GeV, $p_T^{\mathrm{jet}2} > 100$ GeV	4 852	3 924	928
$\not{E}_T > 200$ GeV	3 392	2 719	673
$\min\left[\Delta R(bb)\right] < 1.2$	1 983	1 673	310
Total efficiency	9.8×10^{-2}	0.16	3.2×10^{-2}

Table 5. Events remaining after each step of the event selection at $\sqrt{s} = 14$ TeV. The event categories are similar to those in table 4. The total number of generated events in the inclusive sample is arbitrary.

selected to give adequate statistics for the event selection. The inclusive SUSY sample is split into signal and background, where the signal consists of the events containing at least one Higgs boson (as determined from Monte Carlo truth information). In the last row we give the accumulated total efficiencies of all the cuts. Looking first at table 4, we see that an efficiency of 5.5×10^{-2} is obtained for the case with $M_{\mathrm{SUSY}} = 750$ GeV. This efficiency is more than doubled (0.12) for the case with $M_{\mathrm{SUSY}} = 1$ TeV, since the heavier squarks give harder jets as decay products which leads to more events passing the jet p_T cuts. The larger boost given to the LSP at the end of the decay chain also leads to an increased $\not{E}_T$. The same qualitative features are visible at 14 TeV, as can be read off table 5. Due to the favorable signal statistics at 14 TeV,[6] we can afford slightly harder cuts on $\not{E}_T$ and $\Delta R(bb)$ in this case, something which is also needed to maintain a good background suppression. One should therefore not be discouraged by the somewhat lower efficiencies recorded in this case (4.2×10^{-2} for $M_{\mathrm{SUSY}} = 750$ GeV vs. 9.8×10^{-2} for $M_{\mathrm{SUSY}} = 1$ TeV). The signal efficiencies can be compared to those for the $t\bar{t}$ background, given in table 6, which are at the 10^{-5} level for both energies. It is clear from this table that the hard cuts on the jet p_T and the $\not{E}_T$ distribution are the most important handles available to suppress the background.

As discussed in the previous section, we do not apply any specific cuts to suppress the background from SUSY events that do not involve a Higgs boson. The numbers given in tables 4 and 5 show that nevertheless our event selection gives rise to an improvement also in the ratio of signal events over SUSY-background events. The largest difference in

[6] Going from 7 TeV to 14 TeV, the signal cross section for $M_{\mathrm{SUSY}} = 750$ GeV increases by a factor 14.5, while the $t\bar{t}$ cross section is only increased by a factor 5.

SM $t\bar{t}$ background	7 TeV	14 TeV
Generated events	900 000	2 000 000
$n_j \geq 2$, $n_b \geq 2$	259 110	576 232
$p_T^{\text{jet}1} > 250$ GeV, $p_T^{\text{jet}2} > 100$ GeV	1 120	5 189
$\not{E}_T > 150$ GeV (7 TeV), > 200 GeV (14 TeV)	102	405
$\min[\Delta R(bb)] < 1.5$ (7 TeV), < 1.2 (14 TeV)	12	61
Total efficiency	1.3×10^{-5}	3.0×10^{-5}

Table 6. SM $t\bar{t}$ background events remaining after each step of the event selection at $\sqrt{s} = 7$ TeV and $\sqrt{s} = 14$ TeV. The total number of generated events is arbitrary.

selection efficiency between the SUSY signal and background arises from the typical number of b quarks produced in the two cases, which is larger for the events where Higgs bosons are produced, leading to a stronger reduction of the SUSY background by the jet multiplicity cut. The cut on ΔR also contributes to the difference. This cut has the pleasant "side effect" to enrich the SUSY sample in Higgs events since the jets resulting from $H_1 \to b\bar{b}$ decays are more likely to show up for small ΔR than those from two unpaired b-jets.

4.4 Results

Figure 9 shows the resulting $b\bar{b}$ mass spectra after final event selection for an integrated luminosity of 5 fb^{-1} at 7 TeV. For events with $n_b > 2$ only the b-jet combination minimizing $\Delta R(bb)$ has been included. This reduces effects of combinatorics and increases the sensitivity for discovering resonances in the low mass region. For the scenario with relatively light squarks ($M_{\text{SUSY}} = 750$ GeV) shown in the left plot, we observe two peaks close to the masses of the Z boson and H_1, respectively. There is also a continuous distribution with a tail towards much higher values for $M_{b\bar{b}}$. This results from false pairings, fake b-jets, or from b-jet pairs of non-resonant origin such as t or $\tilde{b}$ decays. The same qualitative features are visible in the signal for $M_{\text{SUSY}} = 1$ TeV (right plot), but the statistics is rather poor due to the low signal cross section. In figure 10 we show the $M_{b\bar{b}}$ distribution at 14 TeV, again for an integrated luminosity of 5 fb^{-1}. Here the signal statistics is much higher, so that a clear distinction of the H_1 resonance from the background should be possible both for $M_{\text{SUSY}} = 750$ GeV (left) and $M_{\text{SUSY}} = 1$ TeV (right).

The same distributions are shown in figures 11 (for the LHC at 7 TeV) and 12 (for 14 TeV), but here with stacked histograms to more closely resemble "real" data. Here we have furthermore split up the inclusive SUSY sample into signal events (displayed in red), characterised by the presence of (at least) one Higgs boson in the decay chain, and the remaining SUSY background events (black). The latter constitutes an additional source of background besides the SM $t\bar{t}$ background (light gray). In figure 11 we see that the most striking feature is the H_1 peak. Although the $t\bar{t}$ background peaks at roughly the same position as the signal, the statistics of signal events should be sufficient for establishing a signal over the background. In the 14 TeV case, figure 12 illustrates the features observed already in figure 10. The H_1 peak stands out clearly above the background distribution, both for $M_{\text{SUSY}} = 750$ GeV and $M_{\text{SUSY}} = 1$ TeV.

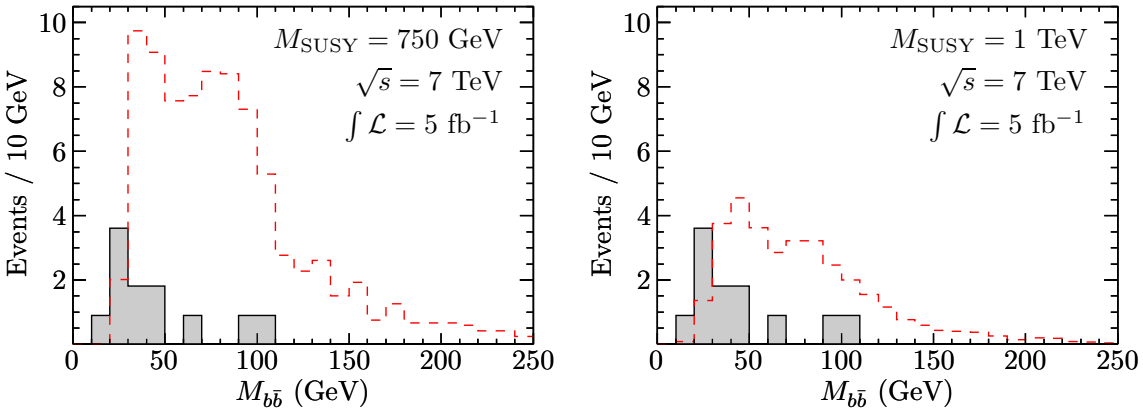

Figure 9. Invariant mass of b-jet pairs after final event selection for the inclusive SUSY sample (red, dashed) and SM $t\bar{t}$ background (solid) at 7 TeV in the modified P4 scenario with $M_{\rm SUSY} = 750$ GeV (left) and $M_{\rm SUSY} = 1$ TeV (right). The histograms have been normalized to an integrated luminosity of 5 fb^{-1}.

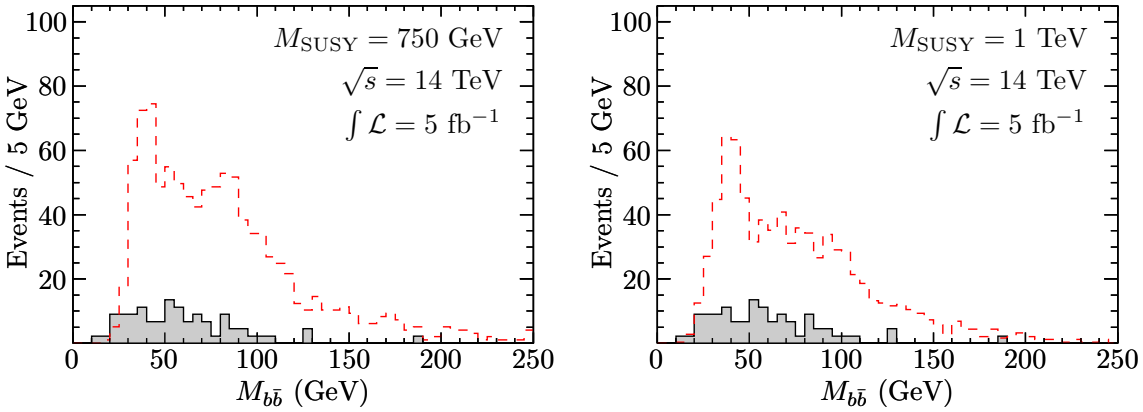

Figure 10. Invariant mass of b-jet pairs after final event selection for the inclusive SUSY sample (red, dashed) and SM $t\bar{t}$ background (solid) at 14 TeV in the modified P4 scenario with $M_{\rm SUSY} = 750$ GeV (left) and $M_{\rm SUSY} = 1$ TeV (right). The histograms have been normalized to an integrated luminosity of 5 fb^{-1}.

With the assumed statistics, no peaks are observed in the $b\bar{b}$ mass spectrum for the heavier Higgs bosons H_2 and A_1. This is mainly due to the smallness of the branching ratios into the $b\bar{b}$ mode because of the open Higgs decay channels. Part of the difficulty in observing the heavier resonances is also a result of selecting the combination minimizing $\Delta R(bb)$ in configurations with multiple b-jets, which favors selection of the light H_1.

In order to obtain an estimate of the significance of the H_1 mass peak we have performed a Gaussian fit to the maximum of the distributions in figures 11 and 12. Table 7 lists the results extracted from the fit for the mean value M_H and the $1\,\sigma$ width ΔM_H of the Gaussian peak. We find that the fitted central values reproduce well the correct H_1 mass for all cases (recall that the input mass used in our numerical simulation is $M_{H_1} = 40$ GeV). The statistical uncertainty on the mean value M_H from the fit is about ± 3 GeV for the LHC energy of 7 TeV and about ± 1 GeV for 14 TeV. This reflects the lower signal statis-

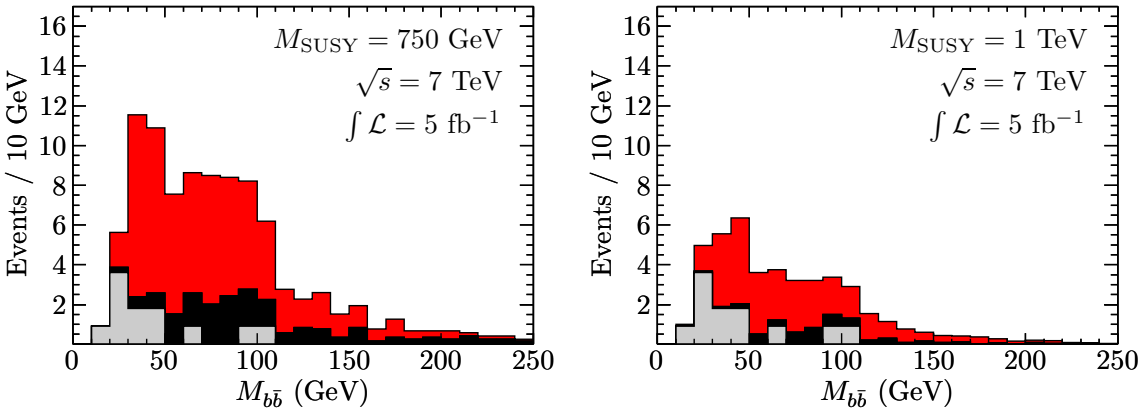

Figure 11. Invariant mass of b-jet pairs for SUSY signal (red), SUSY background (black) and SM $t\bar{t}$ background (light gray) in the modified P4 scenario with $M_{\rm SUSY} = 750$ GeV (left) and $M_{\rm SUSY} = 1$ TeV (right) at 7 TeV for an integrated luminosity of 5 fb^{-1}.

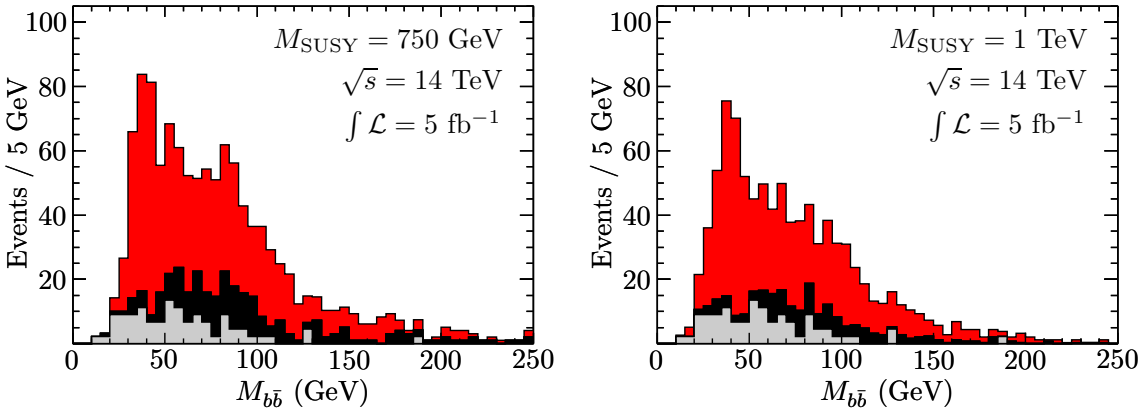

Figure 12. Invariant mass of b-jet pairs for SUSY signal (red), SUSY background (black) and SM $t\bar{t}$ background (light gray) in the modified P4 scenario with $M_{\rm SUSY} = 750$ GeV (left) and $M_{\rm SUSY} = 1$ TeV (right) at 14 TeV for an integrated luminosity of 5 fb^{-1}.

tics available in the low energy running, and the more coarse binning in $M_{b\bar{b}}$ required to observe the peak.

The number of signal and background events in the peak region is obtained by integrating M_{bb} over the interval $[M_H - \Delta M_H, M_H + \Delta M_H]$, corresponding to $\pm 1\,\sigma$ of the Gaussian distribution. As explained above, the combined background includes both the events from SM $t\bar{t}$ and the part of the inclusive SUSY sample containing no Higgs bosons in the cascades. The event numbers are combined into the ratios of signal/background (S/B) and $S/\sqrt{B}$ given in table 7. We use $S/\sqrt{B}$ as a simple illustration for the expected significance and in particular for comparing between the four example cases we consider here and with other theoretical studies using the same criterion. Clearly, claiming an actual discovery would require a more sophisticated statistical treatment. We regard it nevertheless as encouraging that a significance of $S/\sqrt{B} > 5$ is achieved for three of the four cases considered in table 7. The only exception is the case $M_{\rm SUSY} = 1$ TeV for the

$\sqrt{s}$	$M_{\rm SUSY}$ (GeV)	M_H (GeV)	ΔM_H (GeV)	S/B	$S/\sqrt{B}$
7 TeV	750	41.6	12.2	3.4	8.2
7 TeV	1000	37.7	17.6	1.4	3.9
14 TeV	750	39.5	8.0	4.5	29.7
14 TeV	1000	39.4	9.7	4.3	29.3

Table 7. Mean value M_H and width ΔM_H extracted from a Gaussian fit to the $b\bar{b}$ mass peak. The corresponding number of signal (S) and background (B) events is recorded in the $\pm\Delta M_H$ interval around the fitted resonance mass. All results are presented for an integrated luminosity of 5 fb^{-1}.

LHC at 7 TeV, where $S/\sqrt{B} = 3.9$ with 5 fb^{-1}. A somewhat higher luminosity (or a combination of ATLAS and CMS data) would be needed in this case in order to reach a significance $S/\sqrt{B} \geq 5$. The very high significances of about 30 obtained for the 14 TeV case illustrate the qualitative features already observed in the discussion of figures 10 and 12: there should be no problems in establishing a signal in this mass region.

5 Summary and Conclusions

The NMSSM is both theoretically appealing as an extension of the SM and interesting phenomenologically, as its spectrum may contain Higgs bosons with mass much below the limits in the SM or the MSSM. We have investigated an NMSSM scenario with a light CP-even Higgs in the mass range 20 GeV $< M_{H_1} < M_Z$. Scenarios like this may be missed with the standard Higgs search channels at the LHC, in particular due to a potentially large branching ratio of the heavier H_2 state, that has SM-like couplings to gauge bosons, into a pair of light Higgses. We have pointed out that there are good prospects for discovering such a light Higgs boson in SUSY cascade decays at the LHC.

We have performed a Monte Carlo simulation of the signal and the dominant background to the level of fast detector simulation, taking into account also background from other SUSY events that do not involve cascade decays containing a Higgs boson. For our numerical analysis we adapted the "P4" benchmark point proposed for the NMSSM, choosing $M_{H_1} = 40$ GeV as example value for the mass of the light Higgs. Production of squarks and gluinos via the strong interaction at the LHC may give rise to cascade decays involving heavy neutralinos and charginos decaying into lighter ones and a light Higgs. We have investigated the impact of various kinematical variables on discriminating between the inclusive SUSY signal (including events both with and without a Higgs boson in the cascade) and the SM background from $t\bar{t}$ production. A set of simple cuts has been devised that turned out to be efficient for establishing the inclusive SUSY signal. We did not assume any specific knowledge about the background from SUSY events without a Higgs in the cascades. Accordingly, besides favoring events containing the light H_1 by selecting the combination minimizing $\Delta R(bb)$ in configurations with multiple b-jets, we have not applied any particular cuts for suppressing the SUSY background.

Our results show that reconstruction of the decay of the light Higgs into $b\bar{b}$ may be feasible. Such an observation would be a direct experimental sign of the bottom Yukawa

coupling, which is difficult to access in standard search channels. We have investigated two values of the soft SUSY-breaking parameter in the squark sector, $M_{\rm SUSY} = 750$ GeV and $M_{\rm SUSY} = 1$ TeV, while we set the gluino mass parameter to 1 TeV. A modest integrated luminosity of 5 fb^{-1} has been considered for LHC running both at 7 TeV and 14 TeV. We find a statistical significance for the H_1 mass peak of $S/\sqrt{B} \approx 4$ for $M_{\rm SUSY} = 1$ TeV at $\sqrt{s} = 7$ TeV. This significance increases to $S/\sqrt{B} \approx 8$ for $M_{\rm SUSY} = 750$ GeV at 7 TeV and reaches a level of almost 30 for both values of $M_{\rm SUSY}$ at 14 TeV. While the example values that we have chosen for $M_{\rm SUSY}$ and the gluino mass are close to the current search limits from the LHC, the large statistical significance that we have found for the 14 TeV case indicates that there is certainly scope to extend our analysis to scenarios with heavier squarks and gluinos or to scenarios with reduced branching ratios of the neutralinos into Higgs bosons. Since the high-energy run of the LHC is not imminent, we leave a more detailed analysis of this reach for future work.

The results presented here have been obtained in a specific benchmark scenario, but it is easy to see that they are more generally applicable. First of all, the value $M_{H_1} = 40$ GeV used in our numerical analysis was chosen just for illustration. Our results are rather insensitive to the precise value of M_{H_1}. Since the production relies on the decay of heavier SUSY states, with branching ratios largely independent of M_{H_1}, the Higgs production rates remain similar for the whole mass range $M_{H_1} < M_Z$. The event selection and signal identification through $H_1 \to b\bar{b}$ proceeds along similar lines as we have discussed.

Concerning the settings of the other SUSY parameters, our results will be similar for other scenarios fulfilling a few simple criteria: Obviously, the neutralinos and charginos have to be sufficiently lighter than the squarks and gluinos in order to be produced at all in the cascade decays of the latter. The squark decays also provide the hard jets utilized in the event selection. With the present limits from the LHC searches on the masses of the gluino and the squarks of the first two generations this criterion is almost automatically fulfilled for any model of interest. Furthermore, the neutralino and chargino mass hierarchy and mixing character must be such that the squark decays go through heavier neutralinos or charginos, and the decays of the latter into a light Higgs and a lighter neutralino or chargino are open. Such a scenario is disfavored if the LSP is gaugino-like. In order to generate a sufficient number of Higgs bosons in the cascade decays, it is also advantageous for (at least one of) the gauginos to be heavier than the Higgsinos, so that an intermediate Higgsino decay step can be present. In the NMSSM such a situation can be realized quite easily if the LSP is singlino-like.

While the results presented in this paper are based on a rather simple-minded analysis, involving for instance just a fast detector simulation, we nevertheless regard them as very encouraging, motivating a further exploration of the potential for detecting a light non-SM type Higgs in SUSY cascade decays. In fact, there exists the exciting possibility that the discovery of a SUSY signal could go hand in hand with the discovery of one or more Higgs bosons.

Acknowledgments

We are grateful to B. Fuks and F. Staub for valuable assistance with generating the `FeynArts` model file used for parts of this work. We also wish to thank T. Plehn, M. Spira, and S. Brensing for illuminating discussions on the QCD corrections to the squark and gluino production cross sections, and A. Nikitenko, A. Raspereza, and M. Schumacher for giving input on various experimental aspects of our analysis. Finally we thank R. Benbrik, S. Heinemeyer, M. Gomez-Bock, and L. Zeune for interesting and useful discussions. This work was supported by the Collaborative Research Center SFB676 of the DFG, "Particles, Strings, and the Early Universe".

References

[1] H. P. Nilles, *Supersymmetry, Supergravity and Particle Physics*, *Phys. Rept.* **110** (1984) 1–162.

[2] H. E. Haber and G. L. Kane, *The Search for Supersymmetry: Probing Physics Beyond the Standard Model*, *Phys. Rept.* **117** (1985) 75–263.

[3] U. Ellwanger, C. Hugonie, and A. M. Teixeira, *The Next-to-Minimal Supersymmetric Standard Model*, *Phys. Rept.* **496** (2010) 1–77, [arXiv:0910.1785].

[4] M. Maniatis, *The Next-to-Minimal Supersymmetric extension of the Standard Model reviewed*, *Int. J. Mod. Phys. A* **25** (2010) 3505–3602, [arXiv:0906.0777].

[5] ALEPH, DELPHI, L3, OPAL Collaboration, S. Schael *et. al.*, *Search for neutral MSSM Higgs bosons at LEP*, *Eur. Phys. J. C* **47** (2006) 547–587, [hep-ex/0602042].

[6] Particle Data Group, K. Nakamura *et. al.*, *Review of particle physics*, *J. Phys. G* **37** (2010) 075021.

[7] K. Williams and G. Weiglein, *Precise predictions for $h_a \to h_b h_c$ decays in the complex MSSM*, *Phys. Lett. B* **660** (2008) 217–227, [arXiv:0710.5320].

[8] K. E. Williams, H. Rzehak, and G. Weiglein, *Higher order corrections to Higgs boson decays in the MSSM with complex parameters*, *Eur. Phys. J. C* **71** (2011) 1669, [arXiv:1103.1335].

[9] R. Dermisek and J. F. Gunion, *Escaping the large fine tuning and little hierarchy problems in the next to minimal supersymmetric model and $h \to aa$ decays*, *Phys. Rev. Lett.* **95** (2005) 041801, [hep-ph/0502105].

[10] R. Dermisek and J. F. Gunion, *Consistency of LEP event excesses with an $h \to aa$ decay scenario and low-fine-tuning NMSSM models*, *Phys. Rev. D* **73** (2006) 111701, [hep-ph/0510322].

[11] R. Dermisek and J. F. Gunion, *The NMSSM Close to the R-symmetry Limit and Naturalness in $h \to aa$ Decays for $m_a < 2m_b$)*, *Phys. Rev. D* **75** (2007) 075019, [hep-ph/0611142].

[12] R. Dermisek and J. F. Gunion, *The NMSSM Solution to the Fine-Tuning Problem, Precision Electroweak Constraints and the Largest LEP Higgs Event Excess*, *Phys. Rev. D* **76** (2007) 095006, [arXiv:0705.4387].

[13] R. Dermisek and J. F. Gunion, *Many Light Higgs Bosons in the NMSSM*, *Phys. Rev.* **D79** (2009) 055014, [arXiv:0811.3537].

[14] R. Dermisek and J. F. Gunion, *New constraints on a light CP-odd Higgs boson and related NMSSM Ideal Higgs Scenarios*, *Phys. Rev. D* **81** (2010) 075003, [arXiv:1002.1971].

[15] M. S. Carena, J. R. Ellis, A. Pilaftsis, and C. Wagner, *CP violating MSSM Higgs bosons in the light of LEP-2*, *Phys. Lett. B* **495** (2000) 155–163, [hep-ph/0009212].

[16] V. Buescher and K. Jakobs, *Higgs boson searches at hadron colliders*, *Int. J. Mod. Phys. A* **20** (2005) 2523–2602, [hep-ph/0504099].

[17] M. Schumacher, *Investigation of the discovery potential for Higgs bosons of the minimal supersymmetric extension of the standard model (MSSM) with ATLAS*, [hep-ph/0410112].

[18] E. Accomando, A. Akeroyd, E. Akhmetzyanova, J. Albert, A. Alves, *et. al.*, *Workshop on CP Studies and Non-Standard Higgs Physics*, [hep-ph/0608079].

[19] A. Akeroyd, *Searching for a very light Higgs boson at the Tevatron*, *Phys. Rev. D* **68** (2003) 077701, [hep-ph/0306045].

[20] D. K. Ghosh, R. Godbole, and D. Roy, *Probing the CP-violating light neutral Higgs in the charged Higgs decay at the LHC*, *Phys. Lett. B* **628** (2005) 131–140, [hep-ph/0412193].

[21] K. Cheung, J. Song, and Q.-S. Yan, *Role of $h \to \eta\eta$ in Intermediate-Mass Higgs Boson Searches at the Large Hadron Collider*, *Phys. Rev. Lett.* **99** (2007) 031801, [hep-ph/0703149].

[22] M. Carena, T. Han, G.-Y. Huang, and C. E. Wagner, *Higgs Signal for $h \to aa$ at Hadron Colliders*, *JHEP* **0804** (2008) 092, [arXiv:0712.2466].

[23] A. C. Fowler and G. Weiglein, *Precise Predictions for Higgs Production in Neutralino Decays in the Complex MSSM*, *JHEP* **01** (2010) 108, [arXiv:0909.5165].

[24] P. Draper, T. Liu, and C. E. Wagner, *Prospects for Higgs Searches at the Tevatron and LHC in the MSSM with Explicit CP-violation*, *Phys. Rev. D* **81** (2010) 015014, [arXiv:0911.0034].

[25] P. Bandyopadhyay, *Higgs production in CP-violating supersymmetric cascade decays: Probing the 'open hole' at the Large Hadron Collider*, [arXiv:1008.3339].

[26] P. Bandyopadhyay and K. Huitu, *Production of two Higgses at the Large Hadron Collider in CP-violating supersymmetry*, [arXiv:1106.5108].

[27] LEP Working Group for Higgs boson searches, R. Barate *et. al.*, *Search for the standard model Higgs boson at LEP*, *Phys. Lett. B* **565** (2003) 61–75, [hep-ex/0306033].

[28] CMS Collaboration, G. Bayatian *et. al.*, *CMS technical design report, volume II: Physics performance*, *J. Phys. G* **34** (2007) 995–1579.

[29] A. Datta, A. Djouadi, M. Guchait, and F. Moortgat, *Detection of MSSM Higgs bosons from supersymmetric particle cascade decays at the LHC*, *Nucl. Phys. B* **681** (2004) 31–64, [hep-ph/0303095].

[30] K. Huitu, R. Kinnunen, J. Laamanen, S. Lehti, S. Roy, *et. al.*, *Search for Higgs Bosons in SUSY Cascades in CMS and Dark Matter with Non-universal Gaugino Masses*, *Eur. Phys. J. C* **58** (2008) 591–608, [arXiv:0808.3094].

[31] S. Gori, P. Schwaller, and C. E. Wagner, *Search for Higgs Bosons in SUSY Cascade Decays and Neutralino Dark Matter*, *Phys. Rev. D* **83** (2011) 115022, [arXiv:1103.4138].

[32] G. D. Kribs, A. Martin, T. S. Roy, and M. Spannowsky, *Discovering the Higgs Boson in New Physics Events using Jet Substructure*, *Phys. Rev. D* **81** (2010) 111501, [arXiv:0912.4731].

[33] G. D. Kribs, A. Martin, T. S. Roy, and M. Spannowsky, *Discovering Higgs Bosons of the*

MSSM using Jet Substructure, *Phys. Rev. D* **82** (2010) 095012, [arXiv:1006.1656].

[34] K. Cheung and T.-J. Hou, *Light Pseudoscalar Higgs boson in Neutralino Decays in the Next-to-Minimal Supersymmetric Standard Model*, *Phys. Lett. B* **674** (2009) 54–58, [arXiv:0809.1122].

[35] P. Z. Skands *et. al.*, *SUSY Les Houches Accord: Interfacing SUSY Spectrum Calculators, Decay Packages, and Event Generators*, *JHEP* **07** (2004) 036, [hep-ph/0311123].

[36] B. Allanach, C. Balazs, G. Belanger, M. Bernhardt, F. Boudjema, *et. al.*, *SUSY Les Houches Accord 2*, *Comput. Phys. Commun.* **180** (2009) 8–25, [arXiv:0801.0045].

[37] A. Djouadi, M. Drees, U. Ellwanger, R. Godbole, C. Hugonie, *et. al.*, *Benchmark scenarios for the NMSSM*, *JHEP* **0807** (2008) 002, [arXiv:0801.4321].

[38] U. Ellwanger, *Radiative corrections to the neutral Higgs spectrum in supersymmetry with a gauge singlet*, *Phys. Lett. B* **303** (1993) 271–276, [hep-ph/9302224].

[39] T. Elliott, S. King, and P. White, *Supersymmetric Higgs bosons at the limit*, *Phys. Lett. B* **305** (1993) 71–77, [hep-ph/9302202].

[40] T. Elliott, S. King, and P. White, *Squark contributions to Higgs boson masses in the next-to-minimal supersymmetric standard model*, *Phys. Lett. B* **314** (1993) 56–63, [hep-ph/9305282].

[41] T. Elliott, S. King, and P. White, *Radiative corrections to Higgs boson masses in the next-to-minimal supersymmetric Standard Model*, *Phys. Rev. D* **49** (1994) 2435–2456, [hep-ph/9308309].

[42] P. Pandita, *One loop radiative corrections to the lightest Higgs scalar mass in nonminimal supersymmetric Standard Model*, *Phys. Lett. B* **318** (1993) 338–346.

[43] U. Ellwanger and C. Hugonie, *Yukawa induced radiative corrections to the lightest Higgs boson mass in the NMSSM*, *Phys. Lett. B* **623** (2005) 93–103, [hep-ph/0504269].

[44] G. Degrassi and P. Slavich, *On the radiative corrections to the neutral Higgs boson masses in the NMSSM*, *Nucl. Phys. B* **825** (2010) 119–150, [arXiv:0907.4682].

[45] U. Ellwanger, J. F. Gunion, and C. Hugonie, *NMHDECAY: A Fortran code for the Higgs masses, couplings and decay widths in the NMSSM*, *JHEP* **02** (2005) 066, [hep-ph/0406215].

[46] U. Ellwanger and C. Hugonie, *NMHDECAY 2.0: An Updated program for sparticle masses, Higgs masses, couplings and decay widths in the NMSSM*, *Comput. Phys. Commun.* **175** (2006) 290–303, [hep-ph/0508022].

[47] G. Belanger, F. Boudjema, C. Hugonie, A. Pukhov, and A. Semenov, *Relic density of dark matter in the NMSSM*, *JCAP* **0509** (2005) 001, [hep-ph/0505142].

[48] F. Mahmoudi, J. Rathsman, O. Stål, and L. Zeune, *Light Higgs bosons in phenomenological NMSSM*, *Eur. Phys. J. C* **71** (2011) 1608, [arXiv:1012.4490].

[49] D. Eriksson, F. Mahmoudi, and O. Stål, *Charged Higgs bosons in Minimal Supersymmetry: Updated constraints and experimental prospects*, *JHEP* **11** (2008) 035, [arXiv:0808.3551].

[50] D. Stöckinger, *The Muon Magnetic Moment and Supersymmetry*, *J. Phys. G* **34** (2007) R45–R92, [hep-ph/0609168].

[51] U. Ellwanger, *Enhanced di-photon Higgs signal in the Next-to-Minimal Supersymmetric Standard Model*, *Phys. Lett. B* **698** (2011) 293–296, [arXiv:1012.1201].

[52] U. Ellwanger, J. F. Gunion, and C. Hugonie, *Establishing a no-lose theorem for NMSSM Higgs boson discovery at the LHC*, [hep-ph/0111179].

[53] U. Ellwanger, J. F. Gunion, C. Hugonie, and S. Moretti, *Towards a no-lose theorem for NMSSM Higgs discovery at the LHC*, [hep-ph/0305109].

[54] U. Ellwanger, J. F. Gunion, C. Hugonie, and S. Moretti, *NMSSM Higgs discovery at the LHC*, [hep-ph/0401228].

[55] J. R. Forshaw, J. F. Gunion, L. Hodgkinson, A. Papaefstathiou, and A. D. Pilkington, *Reinstating the 'no-lose' theorem for NMSSM Higgs discovery at the LHC*, *JHEP* **04** (2008) 090, [arXiv:0712.3510].

[56] A. Belyaev, S. Hesselbach, S. Lehti, S. Moretti, A. Nikitenko, *et. al.*, *The Scope of the 4 tau Channel in Higgs-strahlung and Vector Boson Fusion for the NMSSM No-Lose Theorem at the LHC*, [arXiv:0805.3505].

[57] S. Choi, D. J. Miller, and P. Zerwas, *The Neutralino sector of the next-to-minimal supersymmetric standard model*, *Nucl. Phys. B* **711** (2005) 83–111, [hep-ph/0407209].

[58] S. Liebler and W. Porod, *Electroweak corrections to Neutralino and Chargino decays into a W-boson in the (N)MSSM*, *Nucl. Phys. B* **849** (2011) 213–249, [arXiv:1011.6163].

[59] T. Hahn, *Generating Feynman diagrams and amplitudes with FeynArts 3*, *Comput. Phys. Commun.* **140** (2001) 418–431, [hep-ph/0012260].

[60] T. Hahn and M. Perez-Victoria, *Automatized one-loop calculations in four and D dimensions*, *Comput. Phys. Commun.* **118** (1999) 153–165, [hep-ph/9807565].

[61] N. D. Christensen and C. Duhr, *FeynRules - Feynman rules made easy*, *Comput. Phys. Commun.* **180** (2009) 1614–1641, [arXiv:0806.4194].

[62] F. Staub, *From Superpotential to Model Files for FeynArts and CalcHep/CompHep*, *Comput. Phys. Commun.* **181** (2010) 1077–1086, [arXiv:0909.2863].

[63] W. Beenakker, R. Hopker, M. Spira, and P. M. Zerwas, *Squark and gluino production at hadron colliders*, *Nucl. Phys. B* **492** (1997) 51–103, [hep-ph/9610490].

[64] J. Pumplin *et. al.*, *New generation of parton distributions with uncertainties from global QCD analysis*, *JHEP* **07** (2002) 012, [hep-ph/0201195].

[65] W. Beenakker, M. Kramer, T. Plehn, M. Spira, and P. M. Zerwas, *Stop production at hadron colliders*, *Nucl. Phys. B* **515** (1998) 3–14, [hep-ph/9710451].

[66] ATLAS Collaboration, G. Aad *et. al.*, *Search for supersymmetry using final states with one lepton, jets, and missing transverse momentum with the ATLAS detector in* $\sqrt{s} = 7$ *TeV pp*, *Phys. Rev. Lett.* **106** (2011) 131802, [arXiv:1102.2357].

[67] ATLAS Collaboration, J. B. G. da Costa *et. al.*, *Search for squarks and gluinos using final states with jets and missing transverse momentum with the ATLAS detector in* $\sqrt{s} = 7$ *TeV proton-proton collisions*, *Phys. Lett. B* **701** (2011) 186–203, [arXiv:1102.5290].

[68] ATLAS Collaboration, G. Aad *et. al.*, *Search for supersymmetry in pp collisions at* $\sqrt{s} = 7$ *TeV in final states with missing transverse momentum and b-jets*, [arXiv:1103.4344].

[69] ATLAS Collaboration, *Search for an excess of events with an identical flavour lepton pair and significant missing transverse momentum in* $\sqrt{s} = 7$ *TeV proton-proton collisions with the ATLAS detector*, [arXiv:1103.6208].

[70] ATLAS Collaboration, G. Aad *et. al.*, *Search for supersymmetric particles in events with lepton pairs and large missing transverse momentum in $\sqrt{s} = 7$ TeV proton-proton collisions with the ATLAS experiment*, [arXiv:1103.6214].

[71] CMS Collaboration, V. Khachatryan *et. al.*, *Search for Supersymmetry in pp Collisions at 7 TeV in Events with Jets and Missing Transverse Energy*, *Phys. Lett. B* **698** (2011) 196–218, [arXiv:1101.1628].

[72] CMS Collaboration, S. Chatrchyan *et. al.*, *Search for Neutral MSSM Higgs Bosons Decaying to Tau Pairs in pp Collisions at $\sqrt{s}$=7 TeV*, [arXiv:1104.1619].

[73] CMS Collaboration, S. Chatrchyan *et. al.*, *Search for supersymmetry in events with a lepton, a photon, and large missing transverse energy in pp collisions at $\sqrt{s} = 7$ TeV*, [arXiv:1105.3152].

[74] CMS Collaboration, S. Chatrchyan *et. al.*, *Search for Supersymmetry in Events with b Jets and Missing Transverse Momentum at the LHC*, [arXiv:1106.3272].

[75] ATLAS Collaboration, *Search for squarks and gluinos using final states with jets and missing transverse momentum with the ATLAS detector in $\sqrt{s} = 7$ TeV proton-proton collisions*, ATLAS-CONF-2011-086.

[76] CMS Collaboration, *Search for supersymmetry in all-hadronic events with α_t*, CMS-PAS-SUS-11-003.

[77] J. Alwall *et. al.*, *MadGraph/MadEvent v4: The New Web Generation*, *JHEP* **09** (2007) 028, [arXiv:0706.2334].

[78] T. Sjöstrand, S. Mrenna, and P. Z. Skands, *PYTHIA 6.4 Physics and Manual*, *JHEP* **05** (2006) 026, [hep-ph/0603175].

[79] S. Ovyn, X. Rouby, and V. Lemaitre, *Delphes, a framework for fast simulation of a generic collider experiment*, [arXiv:0903.2225].

[80] M. Cacciari, G. P. Salam, and G. Soyez, *The anti-k_t jet clustering algorithm*, *JHEP* **04** (2008) 063, [arXiv:0802.1189].

[81] ATLAS Collaboration, G. Aad *et. al.*, *Expected Performance of the ATLAS Experiment - Detector, Trigger and Physics*, [arXiv:0901.0512].

[82] M. Aliev *et. al.*, *– HATHOR – HAdronic Top and Heavy quarks crOss section calculatoR*, *Comput. Phys. Commun.* **182** (2011) 1034–1046, [arXiv:1007.1327].

[83] A. D. Martin, W. J. Stirling, R. S. Thorne, and G. Watt, *Parton distributions for the LHC*, *Eur. Phys. J. C* **63** (2009) 189–285, [arXiv:0901.0002].